POWER ELECTRONICS EUROPE

ISSUE 6 – September 2012 www.power-mag.com

POWER MODULES

Hybrid SiC Power Module with Low Power Loss

THE EUROPEAN JOURNAL FOR POWER ELECTRONICS AND TECHNOLOGY

Also inside this issue


LUXEON

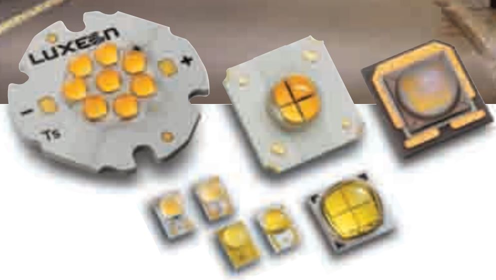

Editor Achim Scharf
Tel: +49 (0)892865 9794
Fax: +49 (0)892800 132
Email: achimscharf@aol.com

Production Editor Chris Davis
Tel: +44 (0)1732 370340

Financial Clare Jackson
Tel: +44 (0)1732 370340
Fax: +44 (0)1732 360034

Circulation Manager Anne Backers
Tel: +44 (0)208 647 3133
Fax: +44 (0)208 669 8013
Email: anne@abdatalog.co.uk

INTERNATIONAL SALES OFFICES

Mainland Europe:
Victoria Hufmann, Norbert Hufmann
Tel: +49 911 9397 643 Fax: +49 911 9397 6459
Email: pee@hufmann.info

Armin Wezel
phone: +49 (0)30 52689192
mobile: +49 (0)172 767 8499
Email: armin@eurokom-media.d

Eastern US
Karen C Smith-Kernc
email: KarenKCS@aol.com
Western US and Canada
Alan A Kernc
Tel: +1 717 397 7100
Fax: +1 717 397 7800
email: AlanKCS@aol.com

Italy
Ferruccio Silvera
Tel: +39 022 846 716 Email: ferruccio@silvera.it

Japan:
Yoshinori Ikeda,
Pacific Business Inc
Tel: 81-(0)3-3661-6138
Fax: 81-(0)3-3661-6139
Email: pbi2010@gol.com

Taiwan
Prisco Ind. Service Corp.
Tel: 886 2 2322 5266 Fax: 886 2 2322 2205

Publisher & UK Sales Ian Atkinson
Tel: +44 (0)1732 370340
Fax: +44 (0)1732 360034
Email: ian@dfamedia.co.uk
www.power-mag.com

Circulation and subscription: Power Electronics Europe is available for the following subscription charges. Power Electronics Europe: annual charge UK/NI £60, overseas $130, EUR 120; single copies UK/NI £10, overseas US$32, EUR 25. Contact: DFA Media, Cape House, 60a Priory Road, Tonbridge, Kent TN9 2BL Great Britain.
Tel: +44 (0)1732 370340. Fax: +44 (0)1732 360034. Refunds on cancelled subscriptions will only be provided at the Publisher's discretion, unless specifically guaranteed within the terms of subscription offer.
Editorial information should be sent to The Editor, Power Electronics Europe, PO Box 340131, 80098 Munich, Germany.

Printed by: Garnett Dickinson.
ISSN 1748-3530

COVER STORY

Hybrid SiC Power Module with Low Power Loss

Mitsubishi Electric has developed a 1.7 kV hybrid SiC power module consisting of 6th generation Si-IGBT and SiC Schottky Barrier Diode (SBD). Adopting SiC-SBD enables a significant power loss reduction during the diode turn-off and IGBT turn-on. And adopting of 6th generation IGBT enables the reduction of the IGBT turn-off loss. Adopting SiC-SBD enables a significant power loss reduction during the diode turn-off and IGBT turn-on. And adopting of 6th generation IGBT also enables the reduction of the IGBT turn-off loss. By using this newly developed chip set, high temperature endure gel, and suitable chip layout, the newly developed hybrid SiC module can be operated at 150°C though the maximum operation temperature of conventional N-series Si modules is 125°C. Compared to the same rating conventional Si N-series module the diode turn-off loss of the newly developed hybrid SiC power module is reduced by 95%, and the IGBT turn-on loss is reduced by 55% respectively in spite of higher operation temperature. When comparing to Si module the IGBT on-state voltage of the hybrid SiC power module is smaller than that of conventional Si module by 0.3 V, but turn-off loss is nearly equal or less in spite of at higher operation temperature. Though the nominal current of the hybrid SiC module is large and the maximum operation temperature is 150°C, it has a wide switching operating area such as the large current turn-off and the short circuit capability. The advantage of SiC in a power module has been confirmed.

Cover supplied by Mitsubishi Electric Europe B.V., Ratingen, Germany

Away from Fossile Energies

A technological transformation of the energy system is still possible, despite current trends. Renewable energy resources and significant potentials for energy efficiency exist virtually everywhere, in contrast to other energy sources, which are concentrated in a limited number of countries. But only a portfolio of more mature renewable energy technologies - including hydro, biomass, onshore wind and solar photovoltaic (PV) - are making sufficient progress. Other key technologies for energy and CO2 emission savings are lagging behind. Particularly worrisome is the slow uptake of energy efficiency technologies, expresses the report on Energy Technology Perspectives (ETP) 2012.

A low-carbon energy system will feature more diverse energy sources. This will provide a better balance than today's system, but it also means that the new system must be more integrated and complex, and will rely more heavily on distributed generation. This would entail increased efficiency, decreased system costs and a broader range of technologies and fuels. Success, however, will critically depend on the overall functioning of the energy system, not just on individual technologies. The most important challenge for policymakers over the next decade will likely be the shift away from a supply-driven perspective, to one that recognises the need for systems integration. Roles in the energy markets will change. Current consumers of energy will act as energy generators through distributed generation from solar PV or waste heat recovery. Consumers will also contribute to a smoother operation of the electricity system through demand response and energy storage. Enabling and encouraging technologies and behaviour that optimise the entire energy system, rather than only individual parts of it, can unlock tremendous economic benefits.

An efficient and low-carbon energy system will require investments in infrastructure beyond power generation facilities. Already, there are bottlenecks in electricity transmission capacity in important markets such as Germany that threaten to limit the future expansion of low-carbon technologies. Systems also need to be operated more intelligently. Better operation of existing heating technologies could save up to 25% of peak electricity demand from heating in 2050, reducing the need for expensive peak generating capacity. Stronger and smarter electricity grids can enable more efficient operation of the electricity system through a greater degree of demand response. Investments in smart grids can also be very cost effective: ETP analysis shows that their deployment could generate up to $4 trillion in savings to 2050 in Europe alone, reflecting a 4:1 return on investment. A majority of these savings could come from a reduction in investment needed for new generation capacity.

Governments need to set stringent and credible clean energy targets. Policies underpinning the targets must be transparent and predictable in order to adequately address and alleviate the financial risks associated with new technologies. Strong policies and markets that encourage flexibility and mitigate risks for investors in these technologies are vital. Ensuring that the true price of energy - including costs and benefits - is reflected in what consumers pay must be a top priority for achieving a low-carbon future at the lowest possible cost. Putting a meaningful price on carbon would send a vital price signal to consumers and technology developers. Phasing out fossil fuel subsidies - which in 2011 were according to ETP almost seven times higher than the support for renewable energy - is critical to level the playing field across all fuels and technologies. Temporary transitional economic incentives can help to create markets, attract investments and trigger deployment. The success of some renewable energy technologies provides evidence that new, emerging technologies can break into and successfully compete in the market place. Solar PV has averaged 42% annual growth globally over the last decade; onshore wind has averaged 27%. As a result of strategic and sustained policy support of early stage research, development, demonstration and market deployment, these technologies have reached a stage where the private sector can play a bigger role, allowing subsidies to be scaled back. System costs for solar PV have fallen by 75% in only three years in some countries. Policy makers must learn from these examples, as well as from the failures in other technologies, as they debate future energy policies. Breakthrough technologies are likely to be needed to help further cut energy demand, and expand the long-term opportunities for electricity and hydrogen, in part to help limit excessive reliance on biomass to reach zero emissions. RD&D efforts that aim to develop such options must start (or be intensified) long before 2050. Power electronics will play an important part in these efforts.

Achim Scharf
PEE Editor

PV Power Generation Exploses

According to the European Photonic Industry Consortium (EPIC) Photovoltaic (PV) industry revenues reached a record $ 93 billion in 2011, a 13.4% increase over $ 82 billion in 2010, and a 150% increase over revenues in 2009. World-wide, 27.4 GW of PV were installed, bringing cumulative PV electrical generation capacity to 68 GW at the end of 2011. Our data show that installations grew by 56% compared to 2010.

Europe remains the leader for deployment, accounting for more than 63% of the PV installations worldwide. About 27% of all the installations took place in Germany. These percentage figures are lower than those for 2010, and they indicate the growing importance of PV markets outside of Europe, and in particular in China.

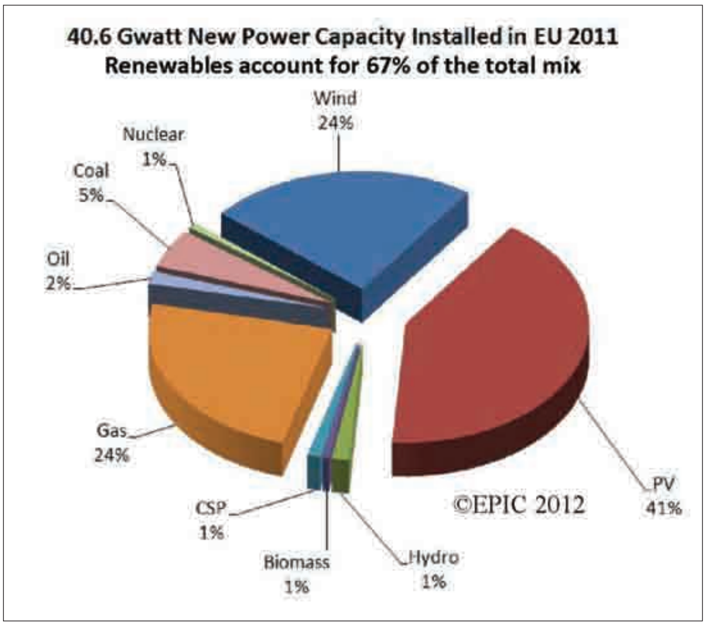

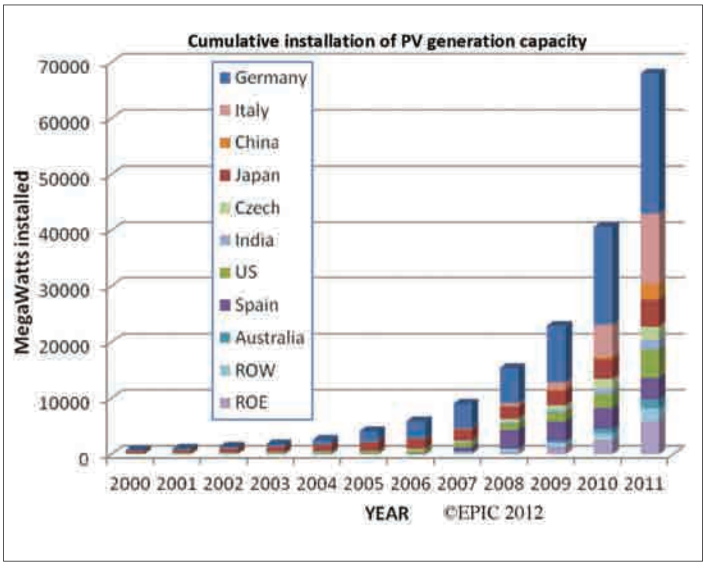

In Europe, 41 GW of electrical generation capacity from all sources were installed in 2011. This can be compared to 57.6 GW in 2010. This decrease is due in part to the economic recession which strengthened in Europe throughout the year. For the first time ever, more PV generating power was installed in Europe than any other energy source, surpassing both natural gas and wind turbine generation. New European PV at 17.3 GW outpaced natural gas installations by 58%. However on a worldwide basis, wind power remains the dominant new renewable energy source with installations of over 40 GW in 2011. By 2011, the cumulative installed PV generating base reached 68 GW. By comparison, this represents about 28% of the installed wind base of 238 GW.

In terms of production, 7.6% more wattage of PV cells was manufactured than generating capacity installed (29.5 GW compared to 27.4 GW). Inventories at the end of 2011 amounted to less than 1 month. Our figure of merit, (the ratio of total sector revenues to installed PV generation capacity) for 2011 improved significantly to $ 3.53 per watt by 24% compared to $ 4.6 per watt in 2010. PV production volume is now dominated by manufacturing in Asia where China and Taiwan now account for about 74% of the world supply. Production by European companies declined sharply in 2011 to less that 6% of the global total. Because many of the remaining companies manufacture some of their products in Asia, the actual amount of manufacturing activity in Europe is even less significant.

www.epic-assoc.com

Global PV Inverter Market to Return to Growth in 2012

According to IMS Research the global PV inverter market shrank marginally in terms of revenues in 2011, but is predicted to return to growth in 2012. Shipments are forecast to grow by almost 25 percent in IMS Research's mid-case scenario; however pricing declines will see revenues grow by just 3 percent this year. "In 2012, suppliers will continue to see high shipment growth but may struggle to see top- and bottom-line growth," commented Ash Sharma, director of the IMS Research PV practice. "Inverter prices will see another double-digit drop in 2012, partly driven by product mix change, and shifts in demand to lower cost countries, but also standard price erosion as major markets stagnate."

The analysis found that in 2011, global inverter shipments grew by more than 12 percent, despite the excess inventory overhang from the prior year, and reached 27 GW, but the European market shrank considerably. Europe's dominance of the PV inverter market is predicted to continue to wane due to its two biggest markets, Germany and Italy, facing significant reductions in their annual installations. "Europe's share of PV inverter shipments and revenues was over 80 percent in 2010; however we forecast this to fall to less than 40 percent in 2016 and revenues not to return to 2011 levels in the next five years. This in itself presents a huge challenge to suppliers, which are mainly European, with the majority of their facilities and customers located in that region," commented Sharma.

Analysis showed that whilst the European outlook is not so bright, the global picture for PV inverter suppliers looks somewhat better; highlighting the fragmenting nature of the industry that now needs to look to emerging markets for future growth. Global shipments are predicted to continue growing at a double-digit rate over the next five years, with revenues

If You Can't Find The Power You Need Here, It Doesn't Exist.

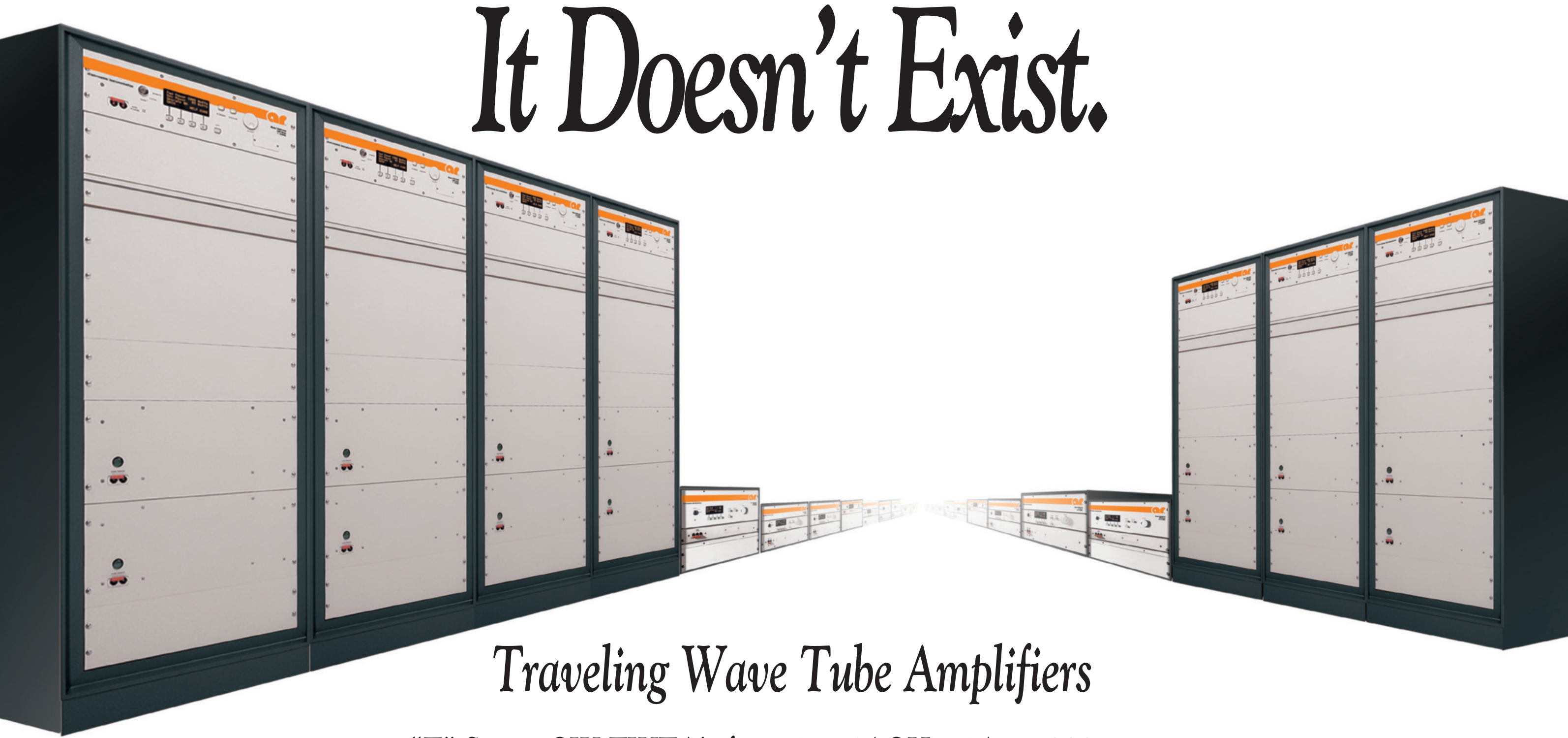

Traveling Wave Tube Amplifiers

"T" Series–CW TWTA's from 1 to 45 GHz. 15 to 2000 watts.
"TP" Series–Pulsed TWTA's from 1 to 18 GHz. 1000 to 10,000 watts.

When it comes to the largest selection of Traveling Wave Tube (TWT) Amplifiers, AR has no equal. We cover a wider range of high-power, broadband amplifiers for your specific test application than any other brand.

CW models also have the capability to faithfully reproduce AM, FM, and pulse modulation input signals. Features that are included at no extra cost are our "Sleep mode" which prolongs the tube life, rugged construction for the rigorous treatment in test labs, modular supplies to reduce repair turn-around, and well thought out digital displays to help you monitor essential amplifier conditions.

So before you choose a look-alike traveling wave tube amplifier, examine all the features and benefits that come along at no extra charge with an AR amplifier. If you want a TWTA that will take you farther, you'll choose the one with the AR logo on it ... the company that stands behind our products with the global service and support that you demand.

www.ar-europe.ie/contact.php

ISO 9001:2008
Certified

ar europe

National Technology Park, Ashling Building, Limerick, Ireland • 353-61-504300 • *www.ar-europe.ie*
In Europe, call ar United Kingdom 441-908-282766 • ar France 33-1-47-91-75-30 • ear Benelux 31-172-423-000

exceeding $9 billion by 2016.

The analysis of the more than 150 suppliers found that the top five remained unchanged, albeit with some slight rankings changings between them. SMA Solar Technology retained its number one position in 2011 despite losing further market share, followed by Power-One, Kaco, Fronius and RefuSOL. IMS Research found however that the biggest market share gainers in 2011 were in fact those outside of the top 10, showing that the industry may not be consolidating just yet. “Start-ups Enphase Energy and SolarEdge were two of the biggest market share gainers in 2011, whilst we also saw considerable gains from Advanced Energy and Emerson,” noted Sharma.

www.imsresearch.com

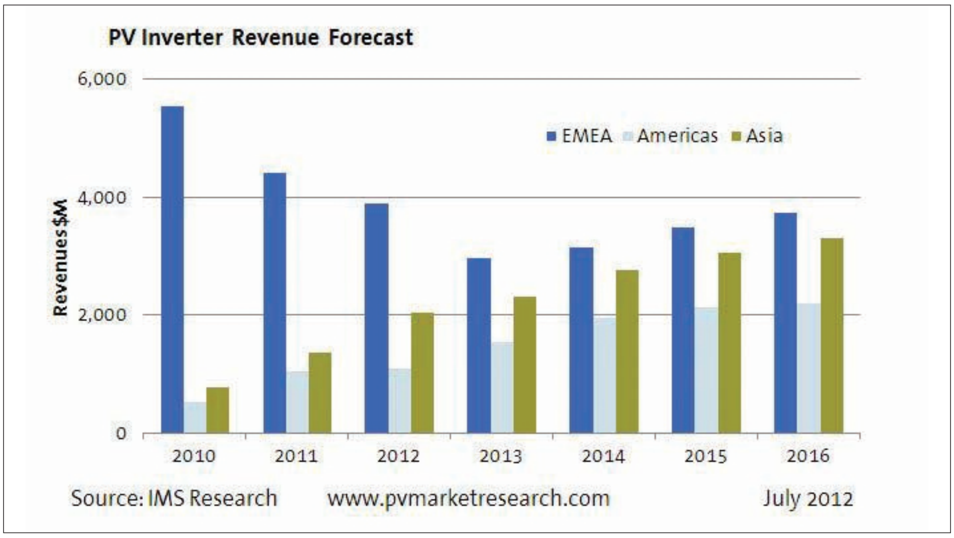

European Reasearch for the Smart Grid

Energy To Smart Grid (E2SG) is a major European energy research project. Six German partner companies (Fraunhofer-Gesellschaft IISB, Infineon Technologies, INSTA Elektro, NXP Semiconductors Germany, RWTH Aachen, Telefunken Semiconductors) are working on new technologies for distributing power from the producer to the end consumer. The aim of the three-year research project is to reduce power losses occurring in energy distribution by 20 percent. E2SG project management is in the hands of Infineon Technologies. The project unites 31 partners in business and research from nine different countries. The German Federal Ministry of Education and Research (BMBF) is supporting the energy research project.

The E2SG project has a total European budget of some Euro 34 million. The German partners from business and research are shouldering Euro 4.9 million, while the BMBF is contributing Euro 4.4 million and ENIAC Joint Undertaking, a public-private partnership focusing on nanoelectronics, is contributing Euro 1.9 million.

In their aim to reduce the amount of energy lost in transmission between the producer and the end user by 20 percent, the German E2SG partners are concentrating their efforts on developing components for the secure, cost-efficient and energy-efficient networking of devices. These devices include electricity meters using specially secured communication technologies for transmitting information regarding energy use from the individual household to the supplier as well as smart power supply units for home appliances, interior and exterior lighting and energy storage.

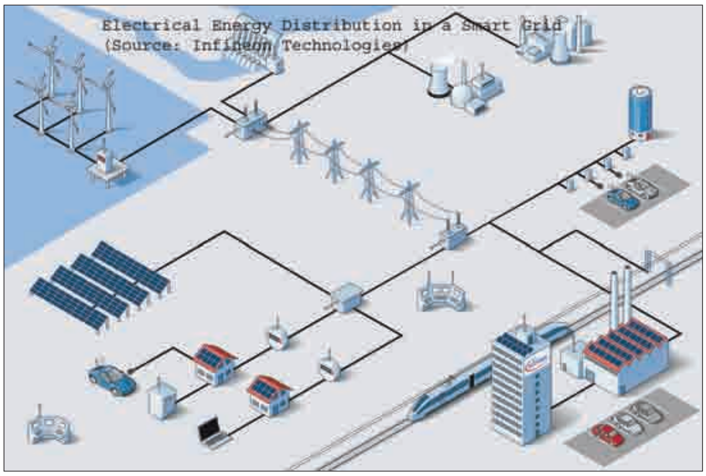

In order to ensure the secure and confidential metering and controlling of energy and to cut energy losses by 20 percent, the components being researched will integrate the latest energy-efficient technologies with grid information and sensor data. The components are to take into account the time when consumers wish to use energy; e.g. by running home appliances at low-tariff-times or when the local photovoltaic system is producing energy. Current security and billing standards as well as comfort levels will not be compromised by these innovative features.

www.iisb.fraunhofer.de

Solutions for Future Energy Supply

Smart Energy Solutions is one of the main themes of electronica 2012, the International Trade Fair for Electronic Components, Systems and Applications in Munich. From November 13 - 16, 2012, the industry's leading manufacturers from around the world will present their solutions and products in the sectors for energy efficiency, energy storage, LEDs and smart grids.

Above all, the future of power grids is expected to be the center of attention. Against the backdrop of the global transition to alternative energy sources and the expansion of power grids, electronica 2012 will present technical solutions for the intelligent supply of power in the future. Leading international executives will also discuss this topic at the CEO Roundtable, the motto of which is "Semiconductor Solutions for Smart Grid Challenges".

Around the world, renewable energies play an increasingly important role in the supply of energy. Given the increased integration of solar and wind energy, energy production is becoming increasingly decentralized and subject to greater fluctuations. To deal with the resulting challenges, grids must not only be expanded, they must also be controlled and monitored more intelligently. Exhibitors at electronica 2012 will present technical solutions that will secure the supply of energy in the future, from components, systems and applications, to sensor technology, the latest network control technical, data-infrastructure solutions and battery-storage systems and intelligent devices for measuring consumption on the part of end consumers (smart meters).

The latest market data also illustrates the extent to which innovations related to smart energy solutions drive the market now and in the future. According to a forecast by the Central Association of the German Electrical and Electronics Industry (ZVEI), volume on the market for electronic components will increase by 5.7 percent to nearly $ 503 billion in 2012. Based on the ZVEI forecast, the most important forces that drive growth are the sectors for environmental protection and energy and resource efficiency. According to the industry association, due to increasing energy costs and guidelines to further reduce CO^2 emissions, these sectors will also ensure continued growth in the years to come.

www.electronica.de

150-mm Silicon Carbide Epitaxial Wafers

Cree announces availability of low micropipe 150-mm 4H n-type Silicon Carbide (SiC) epitaxial wafers for the open market. Larger diameters lowers device cost and enables adoption for customers with existing 150-mm diameter device processing lines. 150-mm epitaxial wafers with highly uniform epitaxial layers as thick as 100 microns are available for immediate purchase. Additionally 100-mm Low Basal Plane Dislocation 4H SiC Epitaxial Wafers are available.

SiC is a high-performance semiconductor material used in the production of a broad range of lighting, power and communication components, including LEDs, power switching devices and RF power transistors for wireless communications. 150-mm diameter single crystal SiC substrates enable cost reductions and increased throughput, while bolstering the continued growth of the SiC industry. "Our ability to deliver high volumes of 100-mm epitaxial

Cree offers besides 100-mm SiC wafers (left) now 150-mm SiC wafers (right) lowering the price for SiC devices

wafers and our latest 150-mm technology continues to raise the standards for SiC wafers," said Dr. Vijay Balakrishna, Cree materials product manager. "Our vertically integrated approach assures customers of a complete solution for high quality 150-mm SiC epitaxial wafers, providing industry leaders within the power electronics market the stable supply they demand."

The company is also offering low basal plane dislocation (LBPD) 100-mm 4H SiC epitaxial wafers. This LBPD material exhibits a total BPD density of 1 cm-2 in the epitaxial drift layer, with BPDs capable of causing Vf drift as low as 0.1 cm-2. "Bipolar devices in SiC have long been held back by forward voltage degradation caused by the presence of BPDs," said John Palmour, CTO, Cree Power & RF. "This Low BPD material enables very high voltage bipolar devices such as IGBTs and GTOs to have improved stability over time. This recent development helps remove roadblocks to commercialization of these extremely high power devices."

www.cree.com, Materials_Sales@cree.com

Powerex Completes New Automated Production Center

Powerex, Inc. announced the opening of a new automated production center capable of producing both Silicon and Silicon Carbide power modules used in inverters for the electric vehicle, aerospace and industrial marketplaces. This project positions Powerex as the leading U.S. manufacturer of medium volume high power semiconductor modules.

A DOE (Department of Energy) grant, awarded in March 2010, provided 70 percent of the funding for the $8.6 million project which increases module production capacity from 17K units produced in 2009 to 100K units in 2015. Looking towards the future of the semiconductor industry, Powerex created this new center to accommodate the production of SiC MOSFET modules.

Since its inception in 1986, Powerex has been manufacturing custom silicon IGBT-based modules. Recently, Powerex offered the first commercially

Examples of Powerex' High Power Silicon and SiC Semiconductor Modules available SiC MOSFET module. These SiC MOSFET modules can operate at temperatures well beyond the temperature limits possible with the traditional silicon IGBT-based modules, allowing for 38 percent lower conduction losses and 60 percent lower switching losses for a total power loss reduction of 54 percent when operated at 20 kHz.

Powerex, Inc. was established in 1986 as a combination of three pioneers in the power semiconductor industry - the Power Semiconductor Divisions of General Electric Company, Westinghouse Electric Corporation and Mitsubishi Electric Corporation. In 1994, Westinghouse sold its shares to General Electric and Mitsubishi Electric. General Electric and Mitsubishi Electric currently share equal ownership of Powerex. The relationship with Mitsubishi allows Powerex to give its customers access to an established supply chain and cutting edge technology. Powerex also manufactures a wide range of semiconductor products at its manufacturing facility in Youngwood/Pennsylvania.

www.pwrx.com

ABB Semiconductors' New Management

ABB Switzerland Ltd announced that Dr. Jürgen Bernauer was appointed as General Manager for Semiconductors effective July 1st, 2012. He succeeds Bernhard Eschermann who has been at ABB Semiconductors for more than five years.

Before joining the Semiconductors unit, Jürgen Bernauer was ABB's General Manager for Gas-Insulated Substations in ABB Switzerland. Mr. Eschermann has assumed his new role as Senior Vice President "Europe for Europe" as part of ABB's strategy 2015+.

www.abb.com/semiconductors

Energy Transfer Electric Vehicles Conference in Nuremberg

The 1st International Energy Transfer Electric Vehicles Conference E|TEV will be held on October 17 2012 as track of the the Electric Drives Production Conference 2012 (E|DPC) at the Nuremberg Convention Center East (NCC Ost) Nuremberg, Germany from October 15 - 18 , 2012.

At E|DPC 2012 the worldwide expert community in application development, production systems and related design aspects of and for automotive and industrial purposes will meet inNuremberg. The aim of the E|DPC and E|TEV Conference 2012 is to bring experts in electrical drive and wireless power transfer system technologies together and to becomethe European platform for national and international exchange in these technologies. The focus of the E|TEV Conference 2012 will be set on the technology of the wirelesspower transfer as well as the market development and needed pre-arrangements. Experts from industry and academia will present latest research achievements, innovative concepts and profound studies. Delegates will find additional information in a comprehensive exhibition and by participating in technical tours to leading manufacturers and research institutes in the field of electric drive train technologies.

www.etev.eu

EconoDUAL™ 3 – Best in class

Highest Power Density with 600 A modules with 650 V / 1200 V / 1700 V IGBT4

The **'Best in class' EconoDUAL™ 3** portfolio with **new PressFIT** auxiliary terminals :

- FF600R07ME4_B11
- FF600R12ME4_B11
- FF600R17ME4_B11

The **EconoDUAL™ 3** modules key applications:

- Construction, commercial and agriculture vehicles
- High performance drives
- Wind applications

The **EconoDUAL™ 3** with optimized features:

- Improved switching characteristics
- Minimized thermal and electrical resistance
- Enhanced mechanical robustness
- PressFIT pins minimizes assembling costs and improves FIT rates

www.infineon.com/highpower

75 W Single-Stage Driver for LED Lighting

Power Integrations' LinkSwitch-PH devices are integrated monolithic switching ICs optimized to provide an isolated, dimmable (up 1000:1), high power factor (PF), constant current driver for LED lighting applications. By integrating the MOSFET and controller plus eliminating the optocoupler and all secondary side feedback components circuit complexity is reduced.

The continuous conduction mode (CCM), variable duty cycle, constant frequency operation provides both high power factor (>0.9), compliance to IEC 6100-3-2 Class C and D harmonic current limits, high efficiency and reduced EMI filtering requirements. Primary side switching current is internally sensed eliminating external current sense resistors. Internal start-up bias current is drawn from a high-voltage current source connected to the DRAIN pin, eliminating the need for external start-up components. The internal oscillator is frequency modulated (jitter) to reduce EMI.

In addition, the ICs have integrated functions that provide system-level protection. The auto-restart function limits dissipation in the device, the transformer and the output diode during overload, output short-circuit and open-loop conditions, while the auto-recovering hysteretic thermal shutdown function disables MOSFET switching during a thermal fault.

LED driver reference design

An isolated LED driver (power supply) has been designed, utilizing a LNK420EG. The RD-290 provides a single constant current output of 2.1 A over an LED string voltage of 29 V to 36 V in a highly efficient, simple and low component count design. The board was optimized to operate over the high AC input voltage range (190 VAC to 300 VAC, 47 Hz to 63 Hz). LinkSwitch-PH based designs provide a high power factor (>0.95) with low harmonic current content. The form factor of the board was chosen to illustrate the simplicity of fitting into standard down light applications.

The LinkSwitch-PH (U1) is a highly integrated primary side controller intended for use in isolated LED driver applications. The LinkSwitch-PH provides high efficiency, high power factor and low THD in a single-stage conversion topology while regulating the output current over a wide range of input (180 VAC - 300 VAC) and output voltage variations typically found in LED driver application environments. All of the control circuitry necessary for these functions plus the high-voltage power MOSFET is incorporated into the device.

Design considerations

The AC supply to the LED driver is protected by fuse. The system input voltage is limited by RV1, D1, R5 and C2 during differential mode line surge voltage events.

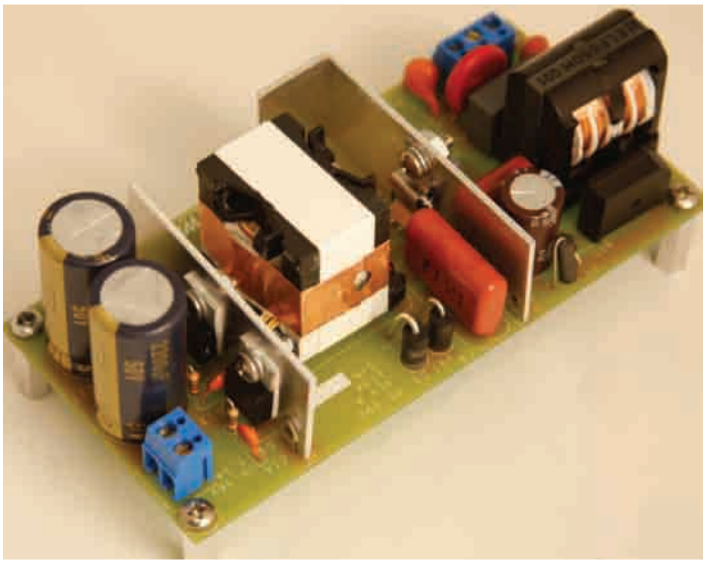

LEFT: RDR-290 LED driver reference design board

The AC input is rectified by BR1. Minimal filter capacitance is used in order to achieve high power factor, low THD and low input current harmonics. Capacitor C8 provides a low impedance source for the primary switching currents. Capacitor C1, common mode choke L1, and differential choke L2, perform EMI filtering while maintaining high-power factor. This input filter network plus the frequency jittering feature of LinkSwitch-PH allows compliance to Class B emission limits. Resistor R3 is used to damp the resonance of the EMI filter, preventing peaks in the conducted EMI spectrum. Capacitors CY1 and CY2 and C13 provide EMI filtering, reducing common mode conducted EMI currents.

Diode D2 and C3 detect the peak AC line voltage. This voltage is converted to a current into the V pin via R6 and R7. This current is also used by the device to set the input over/under-voltage protection thresholds and to provide a linear relationship between input voltage and the output current.

The V pin current and the FEEDBACK (FB) pin current are used internally to control the average output LED current. Constant current (CC) non-dimming applications require 24.9 kΩ ±1% resistance (R9) on the REFERENCE (R) pin.

Diode D6, C9, C10, and R15, create the primary bias supply. This voltage is used to supply current into the BYPASS (BP) pin through D5 and R10. Capacitors C6 and C5 provide decoupling. Capacitor C6 is charged via an internal high-voltage current source connected to the DRAIN pin of U1. This provides the energy to operate U1 until the bias voltage rises and current can be provided via D5.

The output voltage is sensed via R11 which feeds a current in the FB pin proportional to the bias voltage. The bias is related to the output voltage via the bias to output winding turns ratio.

Diode D3 and VR1 clamp due to leakage inductance generated voltage spikes on the drain to a safe level. Diode D4 is necessary to prevent reverse current from flowing through the LinkSwitch-PH device. D4 is low drop diode (Schottky) selected to achieve good efficiency. T1 core size, winding construction and wire gauge are optimized to minimize interwinding capacitance and low AC loss to achieve good efficiency.

Diodes D9 and D10 rectify the secondary winding while capacitors C17 and C18 filter the output. The anode of rectifier diodes are connected to dedicated transformer output windings to assure current sharing. Dedicated RC clamping circuits are placed across each output diode to reduce voltage stress and to limit ringing, reducing radiated and conducted noise. Diodes D9 and D10 are low drop diodes (Schottky), selected to improve efficiency.

The system is protected by a latching over-voltage circuit (D7, C11, C12, VR3, Q1, Q2, R13, R14, R16 and R20). A separate bias voltage was used (via D7 and C11) to reduce the time for the OVP to trigger. Resistor R20 prevents the BP pin being pulled to below ~2 V which limits the dissipation of U1 when the latch is triggered. The OVP circuit operates if the load is not connected and prevents catastrophic failure of the output capacitor. The latch can only be reset by recycling the AC input.

The device is thermally protected in case the system is operated above the specified temperature range.

All in all, RDR-290 is 92.2 % efficient at 230 VAC for a 75 W output design while easily meeting EN61000-3-2 class C limits. Power factor is above 0.95. No primary high-voltage electrolytic bulk capacitor is required, making lifetimes of 50,000 hours practical, even in challenging outdoor environments and at high ambient temperatures. "By greatly increasing the power capability of single-stage conversion, the efficiency and longevity benefits of the single-stage approach can now be applied to industrial and commercial LED lighting - the market that most needs those characteristics", comments product marketing manager Andrew Smith.

A detailled description of this reference design can be found on the link below.

www.powerint.com/sites/default/files/PDFFiles/rdr290.pdf

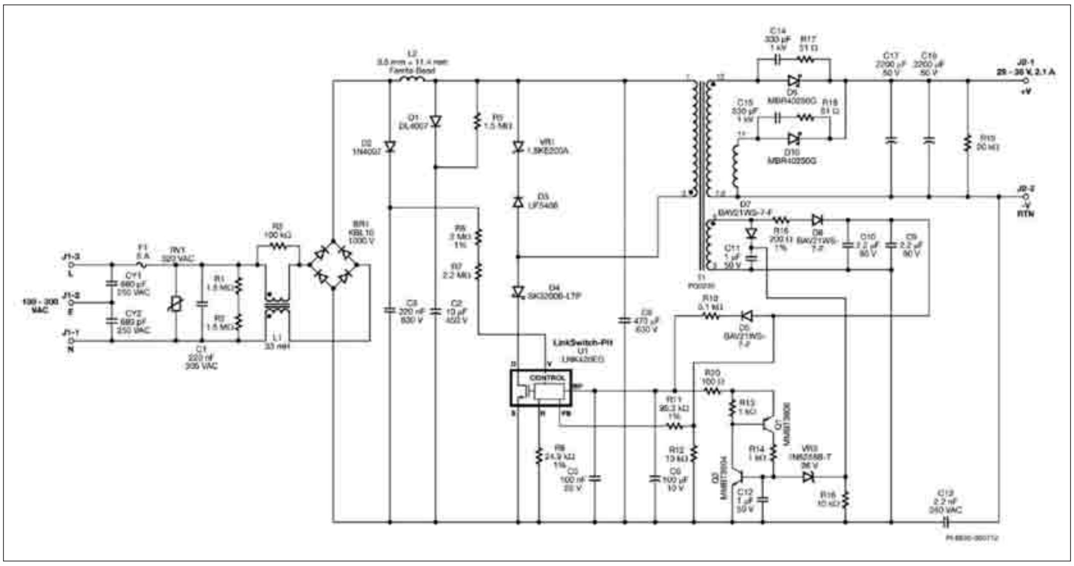

ABOVE: RDR-290 LED driver reference schematic

LED Driver Reference Design Targeting 100 W Incandescent Bulb Replacements

Power Integrations announced DER-323, a reference design for an 18 W, 88%-efficient, non-isolated A19 LED driver based on LNK460VG, a low-profile IC from the company's LinkSwitch-PL family. The design is suitable for a 100 W incandescent bulb replacement and is optimized for low-line (90 VAC to 135 VAC) operation. The circuit is low-cost, requiring only a simple single-sided board and 25 components. No potting is necessary and the transformer is replaced by a low-cost inductor.

DER-323 utilizes a simple buck-boost converter topology that fits easily inside the A19 bulb. The design is EN61000-3-2 (C) compliant and has a high power factor of over 0.98, easily satisfying commercial and consumer compliance requirements. Because LinkSwitch-PL ICs combine both PFC and CC converter functions in a single-stage topology, no electrolytic bulk capacitor is required, resulting in a very long operational life.

Comments Andrew Smith, product marketing manager at Power Integrations: "The lighting industry typically asks for 80% efficiency for drivers targeting 60 W A19 bulb replacements. To achieve viable LED-based replacements for 75 W and 100 W bulbs, much higher efficiency is needed in order to reduce the heat dissipated by the driver. The 88% efficiency of DER-323 satisfies this need and makes the thermal design of the bulb straightforward and inexpensive. DER-323 is also compact, reliable and easy to manufacture thanks to its low component count, single-stage architecture and use of a low-cost inductor rather than a transformer."

www.powerint.com/sites/default/files/PDFFiles/der323.pdf

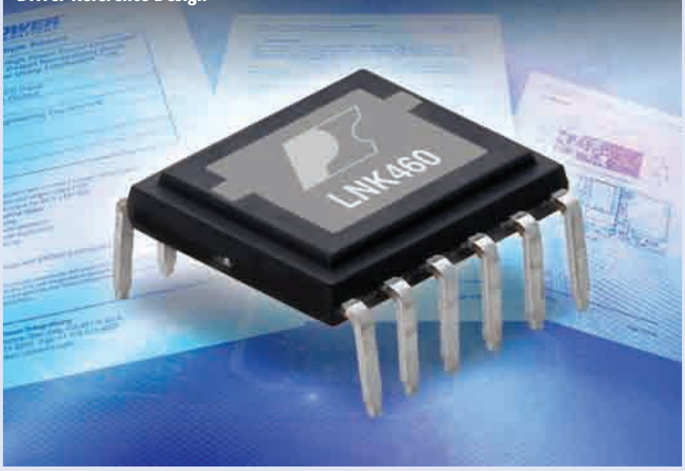

LinkSwitch™-PL low-profile IC LNK460VG in A19 LED Driver Reference Design

Automotive High Current LED Controller

Allegro's A6268 is a DC/DC converter controller that is designed to drive series-connected high power LEDs in automotive applications. It provides programmable constant current output at load voltages and currents limited only by the external components. For automotive applications optimum performance is achieved when driving up to 15 LEDs at currents up to 1 A.

The A6268 can be configured as a standard boost converter or as a supply referenced boost converter. In the supply referenced configuration the load voltage is the difference between the boost voltage and the supply voltage. This difference can be greater than, equal to, or less than the supply voltage, effectively providing a buck-boost capability.

This configuration provides seamless, uninterrupted operation over the wide supply voltage range possible in automotive applications and, because the output is referenced to the positive supply, there is no load current to ground. This ensures that there is no leakage path through the LEDs when in shutdown and no inrush current at power-up.

The A6268 integrates all necessary control elements to provide a cost-effective solution using a single external logic-level MOSFET and minimum additional external passive components.

The LED current is set by selecting an appropriate value for the sense resistor value and using the EN input to provide simple on-off control or for PWM brightness control using a suitable externally generated PWM signal. The LED current can be reduced in a single step by reducing the voltage between the IREF pin and GND to less than 1 V.

Circuit operation

A constant frequency, current mode control scheme is used to regulate the current through the LEDs. There are two control loops within the regulator. The inner loop formed by the amplifier, AS (see the functional block diagram for AS, AC, AE, and AL), comparator, AC, and the RS bistable, controls the inductor current as measured through the switch by the switch sense resistor, RSS.

The outer loop including the amplifier, AL, and the integrating error amplifier, AE, controls the average LED current by providing a setpoint reference for the inner loop.

The LED current is measured by the LED sense resistor, RSL, and compared to the internal reference current to produce an integrated error signal at the output of AE. This error signal sets the average amount of energy required from the inductor by the LEDs. The average inductor energy transferred to the LEDs is defined by the average inductor current as determined by the inner control loop. The inner loop establishes the average inductor current by controlling the peak

A6268 high-current LED driver IC in 16-pin TSSOP package with exposed pad (suffix LP) for enhanced thermal performance

switch current on a cycle-by-cycle basis. Because the relationship between peak current and average current is non-linear, depending on the duty cycle, the reference level for the peak switch current is modified by a slope generator. This compensation reduces the peak switch current measurement by a small amount as the duty cycle increases. The slope compensation also removes the instability inherent in a fixed frequency current control scheme.

The control loops work together as follows: the switch current, sensed by the switch current sense resistor, RSS , is compared to the LED current error signal. As the LED current increases the output of AE will reduce, reducing the peak switch current and thus the current delivered to the LEDs. As the LED current decreases the output of AE increases, increasing the peak switch current and thus increasing the current delivered to the LEDs.

Under some conditions, especially when the LED current is set to a low value, the energy required in the inductor may result in the inductor current dropping to zero for part of each cycle. This is known as discontinuous mode operation, and results in some low frequency ripple. The average LED current, however, remains regulated down to zero. In discontinuous mode, when the inductor current drops to zero, the voltage at the drain of the external MOSFET rings, due to the resonant LC circuit formed by the inductor, and the switch and diode capacitance. This ringing is low frequency and is not harmful.

PWM dimming

LED brightness can be controlled by changing the current, which affects the light intensity. However in some applications, for example with amber LEDs, this will have some effect on the color of the LEDs. In these cases it is more desirable to control the brightness by switching the fixed LED current with a pulse width modulated signal. This allows the LED brightness to be set with little effect on the LED color and intensity and allows direct digital control of the LED brightness.

A PWM signal can be applied to the EN input to enable PWM dimming. The period of this signal should be less than the minimum disable time. During PWM dimming, the A6268 switches the LED current between 100% and 0% of the full current. During PWM dimming, the gate drive is disabled when EN is low. The rate of change of the LED current is also limited, to reduce any large variations in the input current.

Component selection

External component selection is critical to the successful application of the LED driver. Although the inductor, the switching MOSFET, and the output capacitor are the most critical elements, the specification of the rectifying diode and sense resistors should also be carefully considered.

The starting point for component selection is to define the maximum LED current, the voltage across the LEDs, and the input operating voltage range. This then allows the average inductor current under worst case conditions to be calculated. The inductor value is then selected based on the acceptable inductor ripple current. The amount of ripple current will then determine the maximum inductor current under worst case conditions. From this current the switch current sense resistor can be calculated.

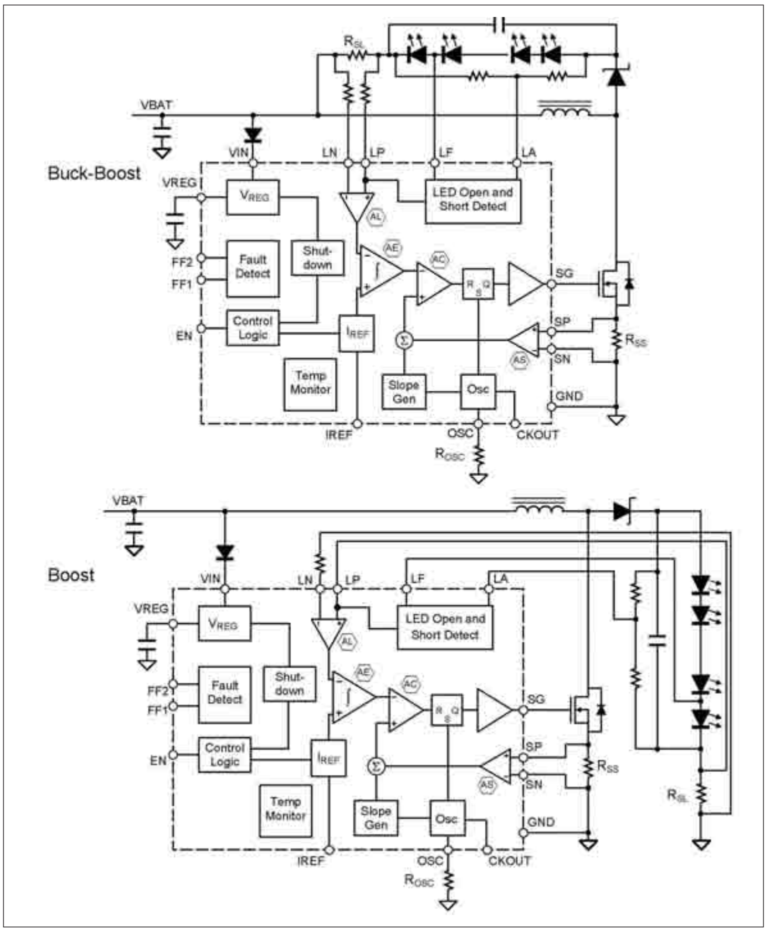

A6268 functional block diagrams in Buck-Boost (upper) and Boost (lower schematic)

External switch MOSFET

A logic-level N-channel MOSFET is used as the switch for the DC/DC converter. In the boost configuration the voltage at the drain of the MOSFET is equal to the maximum voltage across the string of LEDs. In the buck-boost configuration the output voltage is referenced to the positive supply. This means that the voltage at the drain of the MOSFET will reach a voltage equal to the sum of the LED voltage and the supply voltage. Under load dump conditions, up to 90 V may be present on this node. In this case the external MOSFET should therefore be rated at greater than 100 V.

The peak switch current is defined by the maximum inductor current. However, in most cases the MOSFET will be chosen by selecting low on-resistance, which usually results in a current rating of several times the required peak current.

In addition to minimizing cost, the choice of MOSFET should consider both the on-resistance and the total gate charge. The total gate charge will determine the average current required from the internal regulator and thus the power dissipation. When the input voltage reduces below the 5 V regulator drop out level, the gate drive voltage will correspondingly reduce. The level that this occurs at will depend on the average current required for the gate charge. This level will typically occur with an input voltage of around 5.3 V. The effect of a reduced gate drive voltage may be an increase in the on-resistance of the switching MOSFET.

Output capacitor

There are several points to consider when selecting the output capacitor. Unlike some switch-mode regulators, the value of the output capacitor in this case is not critical for output stability. The capacitor value is only limited by the required maximum ripple voltage.

Due to the switching topology used, the ripple current for this circuit is high because the output capacitor provides the LED current when the switch is active. The capacitor is then recharged each time the inductor passes energy to the output. The ripple current on the output capacitor will be equal to the peak inductor current.

Normally this large ripple current, in conjunction with the requirement for a larger capacitance value for stability, would dictate the use of large electrolytic capacitors. In this case stability is not a consideration, and the capacitor value can be low, allowing the use of ceramic capacitors. To minimize self-heating effects and voltage ripple, the equivalent series resistance (ESR), and the equivalent series inductance (ESL) should be kept as low as possible. This can be achieved by multilayer ceramic chip (MLCC) capacitors. To reduce performance variation over temperature, low drift types such as X7R and X5R should be used. The value of the output capacitor will typically be about 10 µF and it should be rated above the maximum voltage defined by the series output LEDs.

More design hints are available under the link below.

www.allegromicro.com/en/Products/Regulators-And-Lighting/LED-Drivers-For-Lighting/A6268.aspx

SEMIKRON
innovation + service

SEMISTACK® RE

Optimized converter for solar and wind

450 kW - 6 MW

- Power density of up to 11.4 kVA/litre
- 2 and 4-quadrant 3-phase converters
- Water-cooled IGBT platform
- Long lifetime

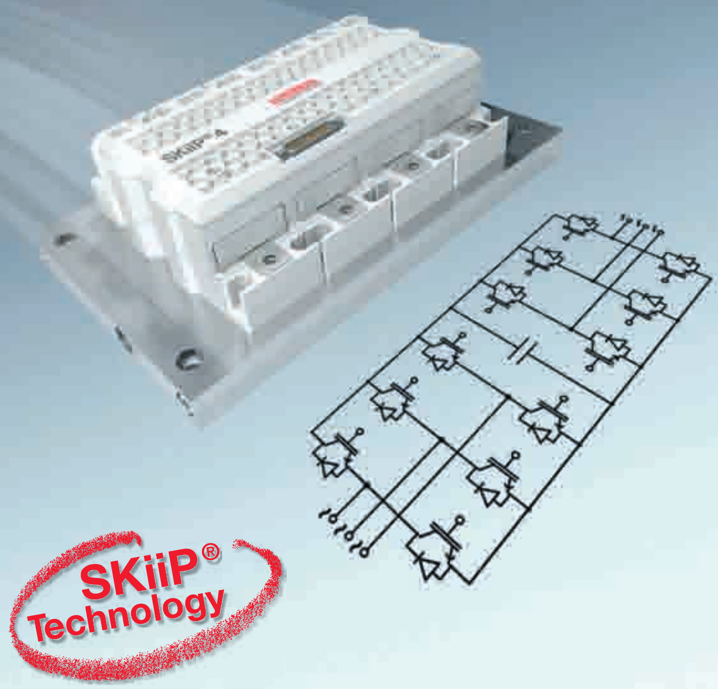

Hybrid SiC Power Module with Low Power Loss

Mitsubishi Electric has developed a 1.7 kV hybrid SiC power module consisting of 6th generation Si-IGBT and SiC Schottky Barrier Diode (SBD). Adopting SiC-SBD enables a significant power loss reduction during the diode turn-off and IGBT turn-on. And adopting of 6th generation IGBT enables the reduction of the IGBT turn-off loss. By using the newly developed chip set, high temperature enduring gel and suitable chip layout, the hybrid SiC module can be operated at 150°C junction temperature. **Shigeru Hasegawa et al, Mitsubishi Electric Corporation, Japan, and Eugen Stumpf, Mitsubishi Electric Europe B.V., Ratingen, Germany**

Recently, Silicon Carbide (SiC) power devices are investigated for the improvement of the conventional Si devices. We have already reported about the electrical characteristics of prototype of the hybrid SiC power module [1]. We have now developed a 1.7 kV hybrid SiC power module with large current capacity and low power loss consisting of newly developed Si-IGBT and SiC-SBD for free-wheeling-diode.

SiC-SBD and Si-IGBT

SiC has a breakdown electric field strength about ten times higher than Si. So the thickness of SiC power chip can be thinner than Si power chip. This enables a significant power loss reduction of the SiC power device in particular for high voltage semiconductors. SiC allows using Schottky Barrier Diodes for high voltage applications, which is not possible with Silicon-SBD due to their high on-state voltage.

SBD is a unipolar device and there is no reverse recovery action during diode turn-off. Since there are no accumulation carriers in a SBD, the conventional reverse recovery loss of the diode is lowered to a negligible level compared with a conventional Si-diode. Moreover, IGBT turn-on switching loss is also reduced because the diode recovery charge is not superimposed to the turn-on current of the IGBT. Figure 1 shows the photo of 1.7 kV SiC-SBD chip (size 6.58 mm x 6.58 mm). The field limiting ring termination structure is adopted which is designed to get the uniform electric field, and more than 1.9 kV blocking voltage is realized at room temperature.

A new (6th) generation 1.7 kV CSTBT™ has been developed by improving the IGBT-cell design and the vertical structure. And the trade-off between the on-state voltage and turn-off switching loss is also improved compared to the conventional N-series Si module.

Figure 5 shows the internal module design. One module consists of four substrates as shown in Figure 6. Each 1.2

Figure 1: SiC Schottky-Barrier diode chip

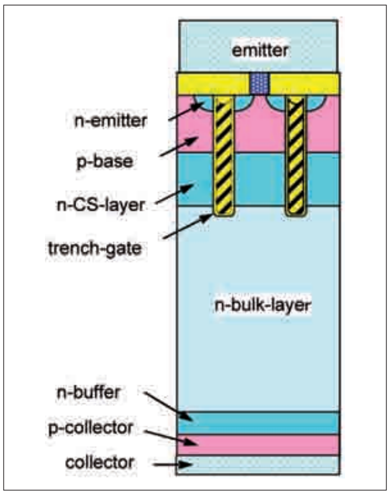

Figure 2: Sixth generation IGBT cell structure

Figure 3: 1.7 kV hybrid power module outline

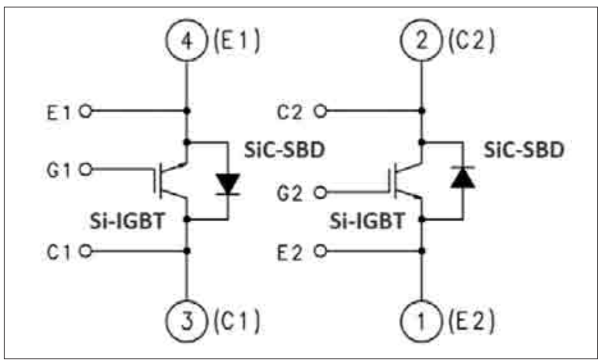

RIGHT Figure 4: 1.7 kV hybrid power module circuit diagram

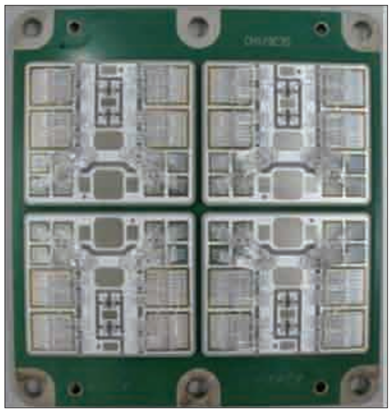

Figure 5: Internal power module design7

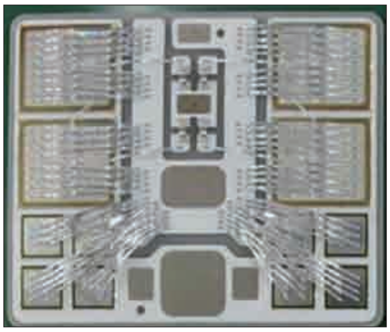

Figure 6: Substrates for the 1.7 kV hybrid power module

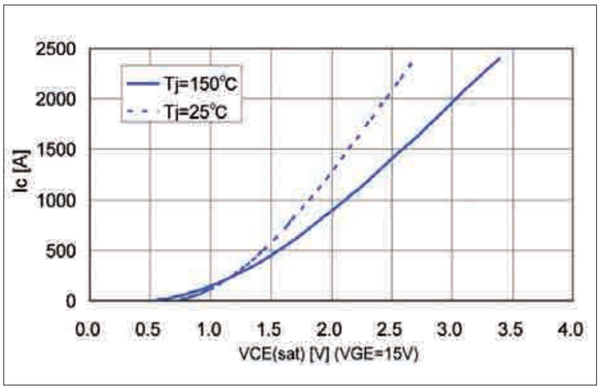

Figure 7: IGBT on-state voltage curve

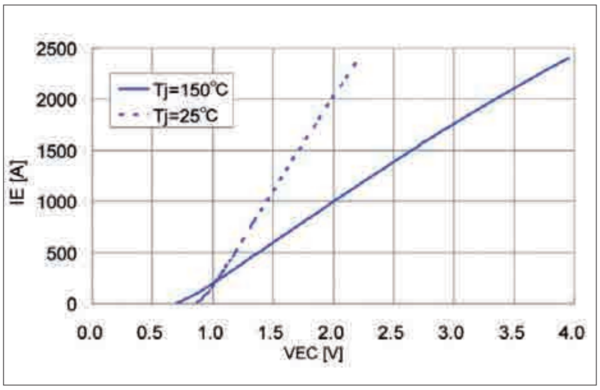

Figure 8: SiC-SBD on-state voltage curve

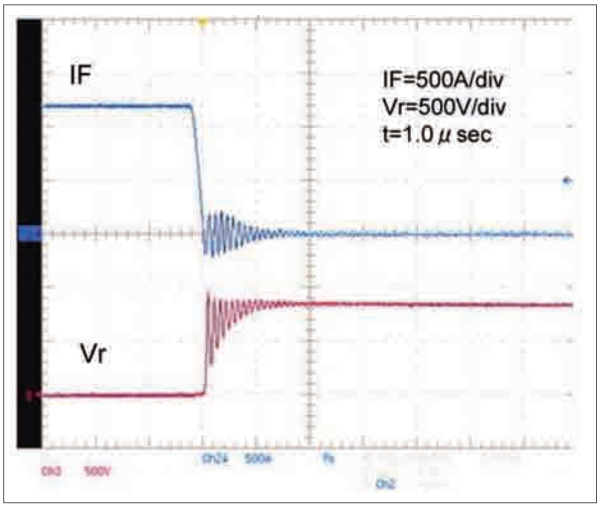

Figure 9: SiC-SBD turn-off

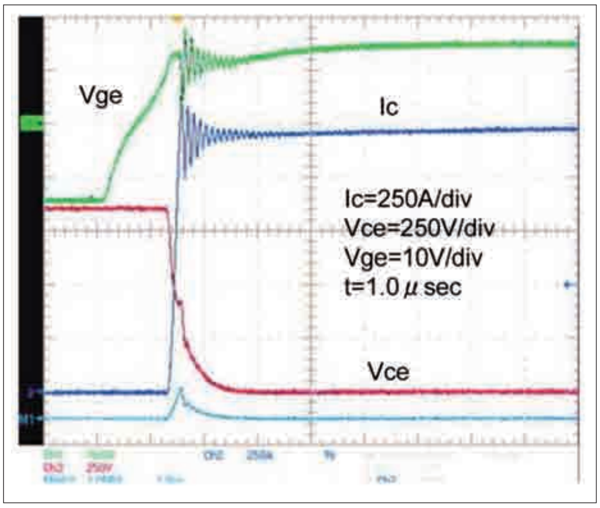

Figure 10: IGBT turn-on

kA arm consists of two substrates. One substrate consists of four Si-IGBTs and eight SiC-SBDs. The quantity and size of Si-IGBT is the same as in the conventional Si module, but the size of SiC-SBD is smaller and the quantity is larger than that of Si module. This depends on low yield of large size SiC chip and improvement of the SiC wafer quality is desired. Many SiC-SBD chips are connected in parallel.

Static and dynamic characteristics

Figure 7 shows the Si-IGBT on-state voltage curves of the hybrid SiC module measured at T_j=25°C and 150°C. The on-state voltage curve of the SiC-SBD is shown in Figure 8. At T_j=150°C the on-state voltage drop at nominal 1.2 kA current of IGBT is V_{CEsat}=2.30V, and that one of SiC-SBD is V_{ec}=2.30V. Both Si-IGBT and SiC-SBD have a positive temperature coefficient. This is advantageous for the large current rating module consisting of many chips in parallel.

Figure 9 shows the SiC-SBD turn-off switching waveform measured at nominal condition (I_F=1.2 kA, Vr=850 V and T_j=150°C). The conventional Si diode is a bipolar device, and there is a reverse recovery charge during the diode turn-off. The SiC-SBD is unipolar device and there is no reverse recovery charge and there is only ringing due to charging the junction capacitance. The Si diode turn-off loss (reverse recovery loss) of the same rating conventional Si N-series at nominal current is 0.22 J/pulse at T_j=125°C, the diode turn-off loss of the developed hybrid SiC module at nominal current is 0.01 J/pulse at T_j=150°C. Compared to the conventional Si module the diode turn-off loss is reduced by 95 % in spite of higher operation temperature.

Figure 10 shows the Si-IGBT turn-on switching waveform at nominal current (1.2 kA) and T_j=150°C. The free-wheeling SiC-SBD features no reverse recovery charge so the Si-IGBT turn-on loss is also reduced. The IGBT turn-on loss of the same rating conventional Si N-series at nominal current is 0.40 J/pulse at T_j=125°C. The IGBT turn-on loss of the developed hybrid SiC module at nominal current is 0.18 J/pulse at T_j=150°C. Compared to the conventional Si module the IGBT turn-on loss of the hybrid SiC module is reduced by 55% in spite of higher operation temperature.

Figure 11 shows the turn-off switching waveform of the 6th generation Si-IGBT at nominal current (1.2 kA) and T_j=150°C. The on-state voltage V_{CEsat} is 2.30 V and turn-off loss is 0.34 J/pulse at T_j=150°C. In the case of the conventional Si module, V_{CEsat} is 2.60V and turn-off loss is 0.37 J/pulse at T_j=125°C. Generally on-state voltage and IGBT turn-off loss have a trade-off relationship. When comparing the IGBT-performance of newly developed hybrid SiC-module with

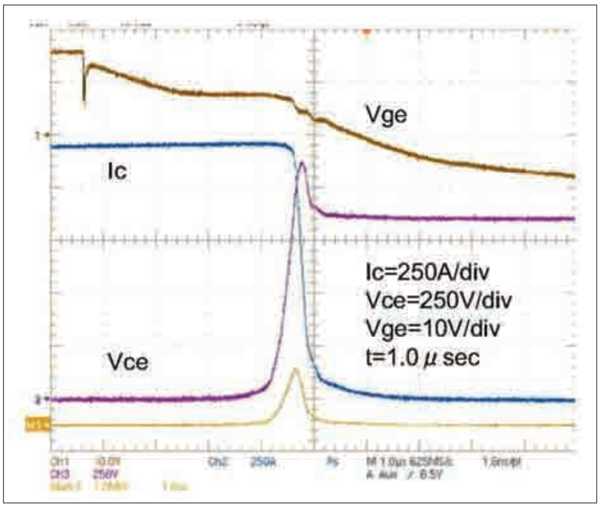

Figure 11: IGBT turn-off

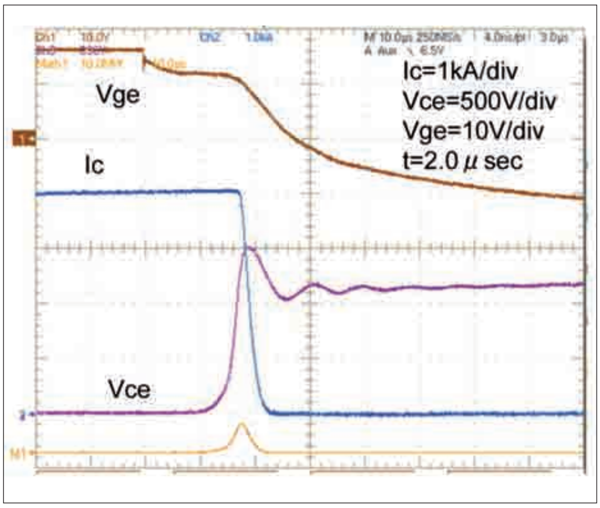

Figure 12: IGBT turn-off capability

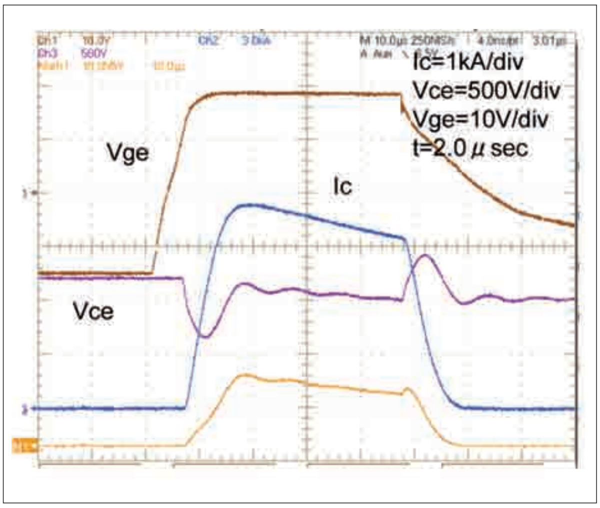

Figure 13: IGBT short circuit capability

conventional Si-module (N-series) the VCEsat is about 0.3 V lower while the turn-off loss is nearly equal or less. Moreover, the operation temperature is higher.

Table 1 shows the comparison of measured characteristics of the hybrid SiC module and the same rating conventional Si N-series module. Despite the higher operation temperature of T_j=150°C of hybrid SiC module compared to T_j=125°C of Si-module a significant reduction of power loss is achieved.

Switching SOA capability

The hybrid SiC module has wide turn-off capability. Figure 12 shows the IGBT turn-off waveform at large current condition at T_j=150°C and DC-link voltage of 1.2 kV. In this test, a current of 4.1 kA, which is more than three times the nominal current, is turned off safely.

Figure 13 shows the short circuit capability at T_j=150°C and V_{cc}=1.2 kV. Although the standard gate voltage is 15 V, the hybrid SiC module has the short circuit capability at V_{GE}=18 V.

Conclusion

Adopting SiC-SBD enables a significant power loss reduction during the diode turn-off and IGBT turn-on. And adopting of 6th generation IGBT also enables the reduction of the IGBT turn-off loss. By using this newly developed chip set, high temperature endure gel, and suitable chip layout, the newly developed hybrid SiC module can be operated at 150°C though the maximum operation temperature of conventional N-series Si modules is 125°C. Compared to the same rating conventional Si N-series module the diode turn-off loss of the newly developed hybrid SiC power module is reduced by 95%, and the IGBT turn-on loss is reduced by 55% respectively in spite of higher operation temperature. When comparing to Si module the IGBT on-state voltage of the hybrid SiC power module is smaller than that of conventional Si module by 0.3 V, but turn-off loss is nearly equal or less in spite of at higher operation temperature. Though the nominal current of the hybrid SiC module is large and the maximum operation temperature is 150°C, it has a wide switching operating area such as the large current turn-off and the short circuit capability. The advantage of SiC in a power module has been confirmed.

Literature

1. Y.Nakayama, T.Kobayashi, R.Nakagawa, K.Hatanaka, S.Hasegawa: Railway motor operation estimation by inverter with SiC-SBD, The 2010 Annual Meeting I.E.E. Japan, 4-139

Item	Si N-series Module Tj=125°C (Si-IGBT,Si-diode)	Hybrid SiC Module Tj=150°C (Si-IGBT,SiC-SBD)
IGBT on-state voltage	2.60V	2.30V
IGBT turn-on loss	0.40J/P	0.18J/P
IGBT turn-off loss	0.37J/P	0.34J/P
Diode on-state voltage	2.30V	2.30V
Diode turn-off loss	0.22J/P	0.01J/P

Table 1: Comparison of power loss between previous N-Series and Schottky-Barrier Diode power module

Railway Inverter with Hybrid SiC Power Module

A newly by Mitsubishi Electric developed railway inverter contains the latest version of large capacity SiC power module consisting of Si-IGBT and SiC-SBD. However, according to the breakdown for energy consumption of the conventional systems for one of the train lines as an example, the railway inverter power consumption is low percentage-wise in energy consumption of the entire railway inverter systems. This means that the potential of the SiC power device is not utilized enough by replacing Si with SiC in the conventional design of railway inverter systems. Motor and Pneumatic Brake show a large ratio in the power consumption which can be possibly reduced by using SiC power device.

The inverter current and the modulation frequency are restricted by power device loss. Using SiC power devices featuring low-loss, the inverter current and the modulation frequency can be increased. To increase the regenerative brake in the high-speed area, traction motor design requires lower impedance. "Voltage by speed (V/F)" of the SiC inverter system is designed to be lower than that of the conventional system in order to preserve the low impedance motor size. Therefore, the motor current of the SiC inverter system is larger than that of the conventional inverter system so that the required torque is maintained. Moreover, the modulation frequency of the SiC inverter system is designed to be higher than the conventional inverter to reduce harmonic current losses in the traction motors.

As the power loss in SiC power modules is much lower than in Si power modules, the cooling effort is also much lower. The foot print of the SiC power module in the railway inverter box (see Figure) is 26 % smaller than that of the Si power module used in the conventional railway inverter box. As a result of applying the SiC power module and other construction improvements, the volume of the railway inverter box is reduced by 42 %, and the mass is reduced by 37 %.

According to the results obtained from the route performance calculation on one of the train lines as an example, application of high frequency asynchronous modulation to a low-impedance traction motor results in expansion of regenerative brake region, which provides a 30 % of energy saving. Based on this scenario, the stable operation was confirmed by the traction system verification test. AS

Applying a SiC power module the volume of a railway inverter box is reduced by 42 % and the mass by 37 % compared to a conventional design with Silicon power modules

Trench Field-Stop IGBT3 Turn-Off

The new Trench-Field-stop devices show significant differences in control characteristics compared to Power MOSFETs. The reason is the large amount of stored charge, which builds up in the conduction mode. This storage effect can be described by an additional element in an equivalent circuit, a capacitance at the output. **Daniel Heer, Reinhold Bayerer, Thomas Schütze, Infineon Technologies AG, Warstein, Germany**

A simple equivalent circuit contains the output characteristics, C_{GC}-, C_{GE}-, and the new C_{CE}-capacitance. This circuit describes principal switching and control characteristics. Characterization of these elements is done by special test configurations, which allow excluding parasitic capacitance of the package. As an additional outcome of the work the stored charge of a 3.3 kV IGBT3 and its dependence on conduction time is received.

Turn-off description of trench field stop IGBT

The turn-off of a standard power MOSFET under inductive load starts with a drop of gate voltage to the threshold for the actual load current. Then the gate voltage stays at that level while the drain voltage is rising and the drain current continues to flow. When the drain voltage reaches the DC-bus voltage the drain current starts to fall controlled by the gate voltage, now drop from the threshold level (Miller plateau) to the off state. The turn-off is completely controlled by the gate voltage - see solid traces of Figure 1. Super-Junction MOSFETs can differ from this behavior.

The Trench-Field-stop IGBT is well suited for inverter circuits, which benefit from low conduction losses. These low losses are achieved by significantly increased carrier density compared to former generations. During turn-off against inductive load, such devices don't require an open MOS-channel all the time to carry the load current. For a short period of time the stored charge is feeding the load current. This behavior occurs at the end of the Miller plateau, where the gate voltage shows a dip in, i.e. the MOS-channel closes while the load current is still running. During this period the collector voltage is rising according to the decay of stored charge. Figure 3 illustrates the turn-off under different load currents.

The dV/dt of the collector voltage varies with the amount of load current in a way

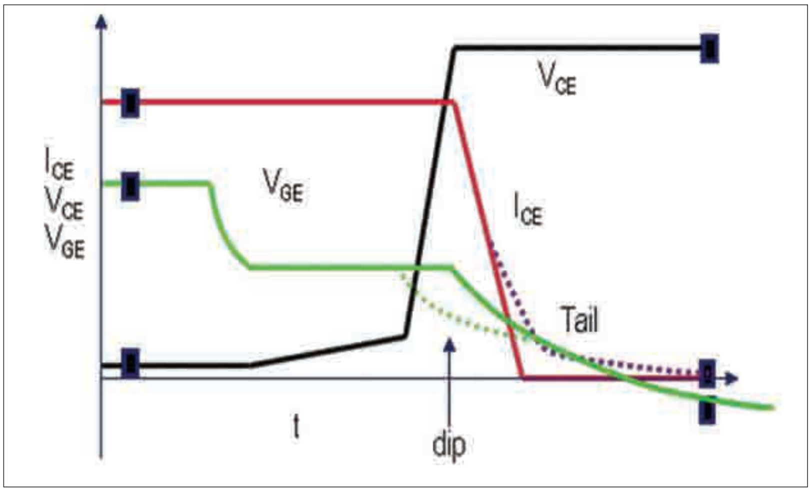

Figure 1: **Turn-off of a MOS-device. Solid traces apply to standard MOSFET, dashed deviations apply for IGBTs. The dip in the gate voltage indicates, that the collector current is carried on by stored charges**

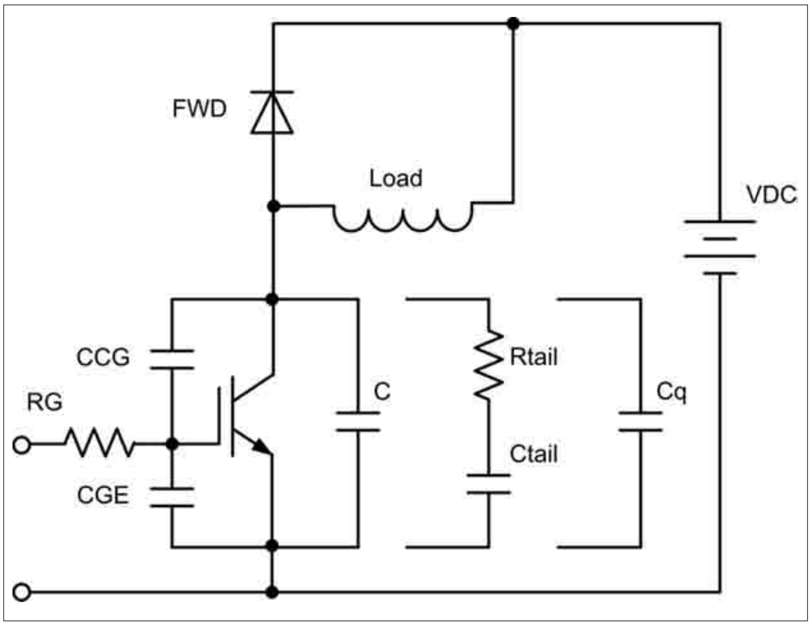

Figure 2: **Equivalent circuit describing the turn-off of a Trench-Fieldstop IGBT under inductive load. The IGBT symbol stands for the static output characteristics $I_{CE}(V_{CE},V_{GE})$. $C_{CG}(V_{CE})$, C_{GE} and C are well known elements for MOSFETs and IGBTs. C_q, C_{tail} and R_{tail} are introduced here to describe the bipolar behavior of the IGBT**

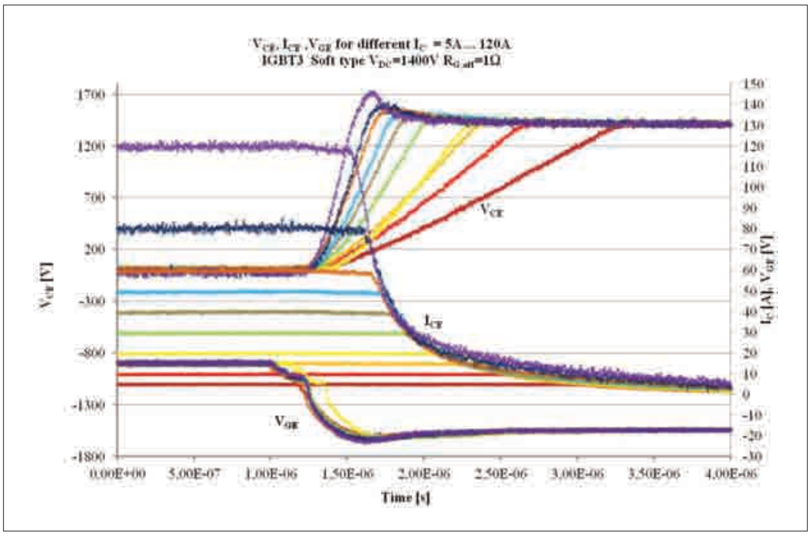

Figure 3: Turn-off of a 3.3kV IGBT3, single chip under different load currents. See the variation in dV/dt with changing collector/load current. At a low gate resistance the gate voltage drops before collector voltage has risen to V_{DC}=1400V

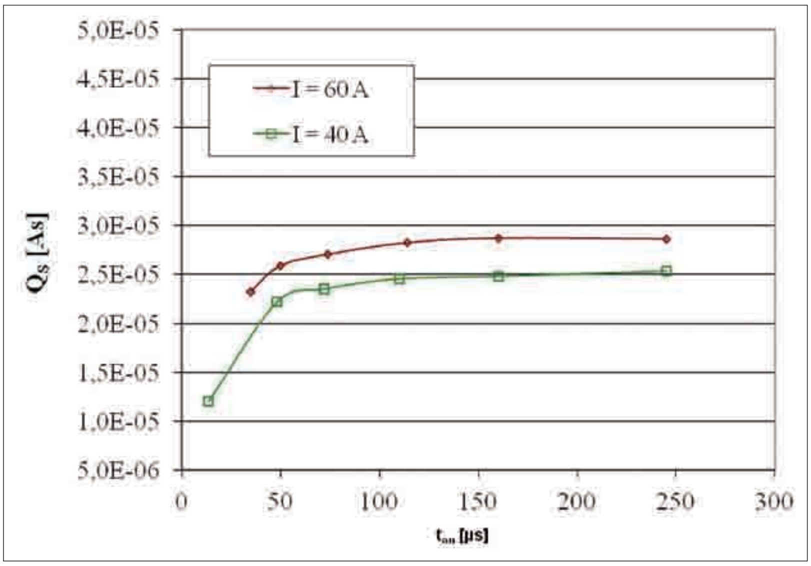

Figure 4: Charge stored in a single 3.3kV IGBT3 as a function of on-time - $Q_S=f_{(ton)}$ (I_C=40 A, t_{on}=14...245 µs and I_C=60 A t_{on}=35...245 µs, V_{DC}=1400 V, R_G=1 Ω)

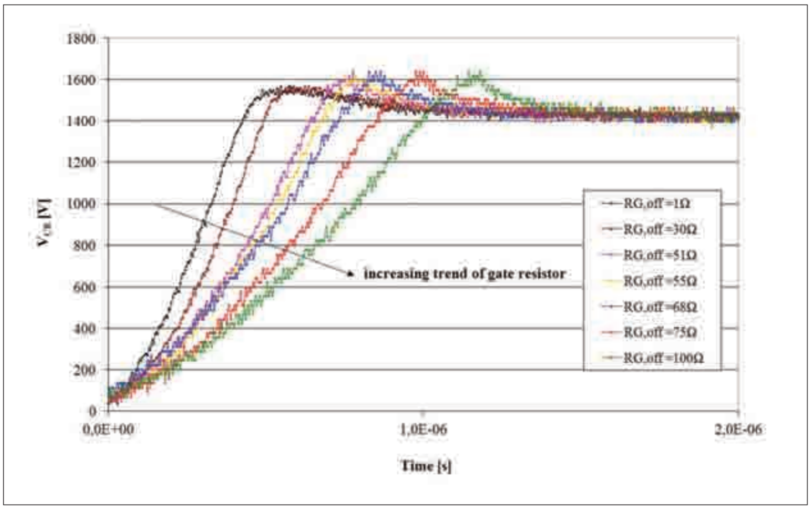

Figure 5: Turn-off of 3.3kV IGBT3, single chip switched with different gate resistors at V_{DC}=1400 V, I_C=60 A, t_{on}=100 µs. See the variation in dV/dt with changing the resistor

similar to loading a capacitor by a constant current. This leads to the equivalent circuit of Figure 2, which represents the switching of a Trench-Fieldstop IGBT by the output characteristics to describe the static characteristics, a collector-gate voltage dependent capacitance a con-stant gate emitter capacitance and an additional output capacitance C_q, which is much larger than the usual junction capacitance between collector and emitter. The tail current is described by an R-C element. The additional output capacitance varies with the amount of stored charge, which depends not only on load current but also on the time the IGBT was in conduction mode. The charge, which is stored in conduction mode and is extracted during collector voltage rise until $V_{CE}=V_{DC}$, is presented in Figure 4 with reference to the on-time of the IGBT.

A further influence of the stored charge on the switching behavior can be shown by variation of the gate turn-off resistance. Figure 5 illustrates the turn-off under different gate resistors. For gate resistors ranging from 1 to 30 Ω, the dV/dt of the collector voltage is constant. The dV/dt is intrinsically limited. The reason is the stored charge controlling the voltage rise. For gate resistors of more than 30 Ω the dV/dt becomes reduced and controlled by the gate resistor RG. The Miller plateau is stretched. During this Miller plateau a significant amount of stored charge is withdrawn, resulting in a higher dI/dt during current fall. This can be detected by an increased over-voltage in Figure 5.

The additional output capacitance C_q in Figure 2 shall describe the self limitation of dV/dt and the effect of stored charge whereas $C_q(V_{CE})$ is a function of $V_{CE(t)}$. During turn-off the collector current divides into MOS-channel and stored charge current. The amount of the MOS-Channel current can be detected by measurement of gate emitter voltage and calculated using the transfer characteristics of the IGBT. The difference between collector current and the MOS-channel current is the share of the stored charge. In the phase of turn-off where the MOS-channel current is negligible (for low R_G) the output capacitance C_q carries the whole load current and determines the dV/dt. The characterization of C_q for the whole range of gate resistors, currents, V_{DC} and t_{on} allows to describe the turn-off with respect to more or less stored charge. As an example this calculated capacitance for different load currents is presented in Figure 6 with reference to the collector voltage of the IGBT.

For the characterization of the IGBT a test setup, which prevents package capacitances, was used. Figure 7 shows a sectional view of

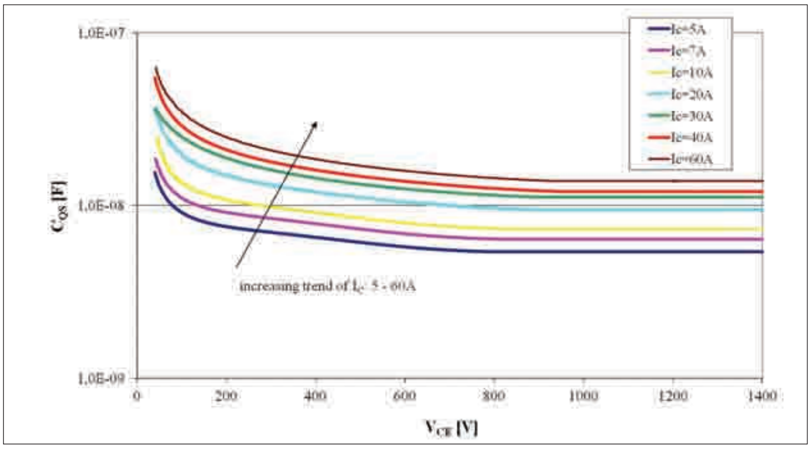

RIGHT Figure 6: Calculated output capacitance C_q for different load currents as a function of the collector voltage (V_{DC}=1400 V, R_G=1 Ω)

the IGBT on the substrate and the circuit diagram for the test. Only one IGBT chip without free-wheeling diode was tested. This reduced the total capacitance which was charged and discharged during dV/dt of the collector voltage and no paralleling effects between two or more IGBTs occured. For the measurement of the true gate emitter voltage the internal gate resistor was shorted. This test setup allowed a pure characterization of the static and dynamic parameters without influence of parasitic package capacitances.

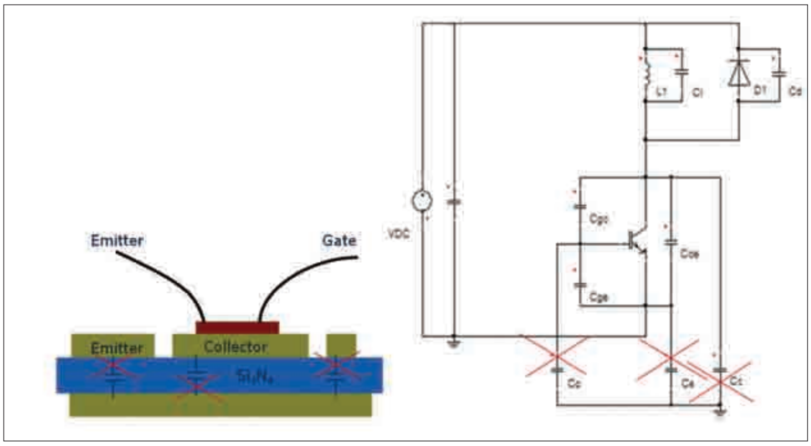

LEFT Figure 7: Sectional view of the IGBT on the substrate (left) and test circuit diagram (right)

Conclusion

A simple behavior model is presented which is easy to establish by characterization and implementation in circuit simulators. It allows better understanding of gate drive and turn-off characteristics of new IGBT generations. The model is applied to the recently introduced 3.3kV IGBT3.

Infrared Determination of Junction Temperature and Switching Losses

Junction temperature of power MOSFETS is one of the major criteria to obtain temperature derating curves for power converters. It is quite evident that the hottest spot temperature on the lead and case (package) areas of a power MOSFET is typically a couple of degrees less than the junction temperature. This hottest spot temperature can be accurately measured by an infrared camera without the heat flow intrusion.

Alexander Asinovski, Murata Power Solutions Inc., Mansfield, Mass., USA

In order to keep the junction temperature (Tj) within specifications, allowable drain (leads) temperature (T_D) is often calculated by the formula:

$$T_D = Tj - Pj * \theta_{JD}, \quad (1)$$

where Pj is the total heat power generated inside the package (includes conduction losses, switching losses and gate losses), θ_{JD} is the junction-to-drain (leads) thermal resistance, which is a package related parameter defined by the MOSFET manufacturers in their data sheets. Typical values of θ_{JD} for some standard power MOSFET packages are shown in Table 1.

If for example, a MOSFET in an SO8 package (θ_{JD}=15 K/W) that dissipates Pj=1 W of power which must maintain a junction temperature below 125°C, then the measured drain temperature must not exceed 110°C according to (1) : T_D =125°C - 1 W * 15 K/W = 110°C.

Using equation (1) implies that Pj can be determined under any operational condition and also that the total power generated inside the package is dissipated to ambient through the drain leads. In reality, the accuracy of the Pj calculation is relatively low because switching losses in the MOSFET cannot be calculated accurately enough. Also since a portion of the Pj is dissipated to ambient through the MOSFET package, actual heat flow through the drain leads is smaller than Pj which presents another source of error while using equation (1).

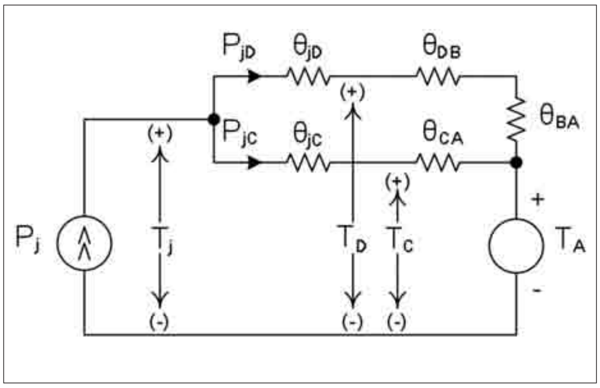

Figure 1: MOSFET thermal model - total heat Pj generated in the MOSFET is dissipated to ambient through two parallel branches: junction-drain (leads)-PCB-ambient and junction-case (package)-ambient

Method for determining a MOSFET junction temperature and switching losses

The objective of this article is to present a method for determining a MOSFET junction temperature and switching losses based on the given thermal resistances and lead and case (package) temperature measurements. In order to develop such a technique let us consider the MOSFET thermal model in Figure1 which is a modification of the model used in [1].

According to this model, the total heat generated in the package, represented by a current source Pj, flows to ambient through two parallel branches: junction-drain (leads) -PCB-ambient ("drain" or "lead" branch, labeled Pj_D) with θ_{JD} - junction-to-drain thermal resistance, θ_{DB} - drain-to-PCB thermal resistance and θ_{BA} - PCB-to-ambient thermal resistance, and junction-case (package)-ambient ("case" or "package" branch, labeled Pjc) with θ_{JC} - junction-to-case thermal resistance and θ_{CA} - ca se-to-ambient thermal resistance. Also in Figure1, T_c is the case temperature and T_A is the ambient temperature represented by a voltage source.

Applying conventional electrical circuit analogy to the diagram in Figure.1 and Ohm's law, we obtain the following

Thermal Resistance	Package Type					
	DirectFET	PowerPAKSO8	DPAK	D2PAK	LFPAK	SO8
θ_{JD}, K/W	1	1.5	1.5	1.5	2	15

Table 1: Typical values of junction-to-drain (leads) for some standard power MOSFET packages

equations for the heat portions Pj_D and Pjc flowing through the respective “drain” and “case” branches:

$$Pj_D = Pj/(1+ \theta_D/\theta_C), \quad (2)$$

$$Pjc = Pj/(1+ \theta_C/\theta_D), \quad (3)$$

where $\theta_D = \theta_{JD} + \theta_{DB} + \theta_{BA}$ (total “drain” branch thermal resistance) and $\theta_C = \theta_{JC} + \theta_{CA}$ (total “case” branch thermal resistance) so that total heat flow Pj is:

$$Pj = Pj_D + Pjc. \quad (4)$$

Applying Ohm’s law to the series combinations of thermal resistances in each branch of the diagram in Figure 1 we get two equations for junction temperature Tj:

$$T_j = T_D+(T_D-T_A)^* \theta_{JD} /(\theta_{DB}+ \theta_{BA}) = T_D+(T_D-T_A)^* \theta_{JD} / \theta_{DA}, \quad (5)$$

$$T_j = Tc+(Tc-T_A)^*\theta_{JC} / \theta_{CA}. \quad (6)$$

Both equations (5) and (6) do not contain heat power Pj and each of them can be used for calculating the junction temperature Tj as long as the case, the drain, ambient temperatures and thermal resistances of the package are known.

If we apply these equations to a typical SO8 power MOSFET with thermal resistances θ_{CA} = 380 K/W, θ_{JC} = 18 K/W, θ_{JD} = 15 K/W and θ_{DA} =20 K/W (given in [1]), substituting these values into equations (2) and (3) we obtain:

$$Pj_D/Pj = 1/[1+(15+20)/(18+380)]=0.92 \quad (7)$$

$$Pjc/Pj = 0.08. \quad (8)$$

In other words, 92% of total power generated in the silicon is dissipated to ambient through the drain and the remaining 8% - through the case. Another important observation is that θ_{CA} is much greater than any other thermal resistance in the system, which makes the second term in equation (6) relatively small. Assuming Tc=125°C and T_A=85°C for the set of parameters given above, the junction temperature according to (6) is Tj = 125+(125-85)*18 / 380=126.9°C. This is only 1.9 K greater than the case temperature. Using equation (5) to calculate the drain temperature, we obtain $T_D = (Tj + T_A^* \theta_{JD} / \theta_{DA})/(1+ \theta_{JD} / \theta_{DA})$ = (126.9+85*15/20)/(1+15/20) =108.9°C.

This temperature is lower than the case temperature by 16.1°C. This implies that for an SO8 power MOSFET with θ_{JD} being on the same order as θ_{DA} and with θ_{CA} being much greater than θ_{JC}, the drain temperature tends to be lower than the case temperature, not only that but the plastic case temperature is an accurate representation of the junction temperature. According to the measurement results in [1] the difference between Tj and Tc for SO8 packages is typically 1-3 K. If we use the same equations for other MOSFET packages like PPAKSO8, D2PAK, DPAK and LFPAK with low junction-to-drain thermal resistances θ_{JD} (see Table 1), both the drain and case temperatures are close to the junction temperature Tj. For DirectFET type MOSFETs with metal case θ_{JD} is even lower and, according to (5), the drain temperature is an accurate representation of the junction temperature.

For a more accurate Tj calculation based on (5), parameter θ_{DA} unavailable from MOSFET data sheets can be determined as follows. According to Figure1 junction-to-ambient thermal resistance θj_A , provided in the MOSFET data sheets, is a parallel combination of θ_D and θ_C resistances and $\theta_{DA} = \theta_D - \theta J_D$. Applying this to the diagram in Figure1 we can get:

$$\theta_{DA} = \theta j_A/(1- \theta j_A/ \theta_C) - \theta_{JD}. \quad (9)$$

Taking into account that θ_C is approximately one order greater than θj_A, equation (9) can be rewritten as:

$$\theta_{DA} \approx 1.1^* \theta j_A - \theta_{JD}. \quad (10)$$

Substituting (10) into (5) we get:

$$Tj \approx T_D+(T_D-T_A)^* \theta_{JD} / (1.1^* \theta j_A - \theta_{JD}), \quad (11)$$

where all the thermal resistance values are available from the data sheets.

The junction temperature was calculated above based on parameters specified on the component data sheet and temperature measurements taken from the device under test conditions. A conventional drain (lead) and case (package) temperature measurement technique is based on the thermocouples placement on the package and on the lead areas. The measured temperatures with the thermocouples are lower than actual temperatures for two reasons: first, the thermocouple itself works as a heat sink cooling the device down and second, its physical placement is critical when trying to determine the hottest temperature of the device. A more accurate temperature measurement method is the use of an infrared camera which determines the hottest spot temperature in the areas of interest (case and lead) without the heat flow intrusion.

As soon as the junction temperature Tj is determined, total power Pj generated in the silicon can be calculated by the formula:

$$Pj = (Tj - T_A) / \theta j_A, \quad (12)$$

where θj_A- junction-to-ambient thermal resistance is available from the MOSFET data sheets. Pj can also be calculated based on equation (2) and junction-to-drain thermal resistance θ_{JD} which is also available from the MOSFET data sheets:

$$Pj = (1+ \theta_D/\theta_C)^*(T_D - T_A) / \theta_{JD}. \quad (13)$$

θ_D and θ_C are not available from the data sheets but since θ_C is approximately one order greater than θ_D, equation (13) can be rewritten as:

$$Pj \approx 1.1^*(T_D - T_A) / \theta_{JD}. \quad (14)$$

After Pj is determined, switching losses Psw can be calculated in the conventional way:

$$Psw = Pj - Pdc - Pg = Pj - I_{rms}^2 * Rds_{on} - Q * V_g * F_{sw}, \quad (15)$$

where Pdc - conduction (DC) losses, Pg - gate drive losses, I_{rms}- RMS value of drain current, R_{dson} - MOSFET ON-resistance, Q - total gate charge, V_g - peak gate voltage, F_{sw} - switching frequency. For a square wave drain current with peak I_{pk} and duty cycle D, $I_{rms}^2 = I_{pk}^2 * D$.

Results

From the above analysis based on the thermal model in Figure1 it is quite evident that the hottest spot temperature on the lead and case (package) areas of a power MOSFET is typically a couple of degrees Celsius less than the junction temperature. This hottest spot temperature can be accurately measured by an infrared camera without the heat flow intrusion.

A more accurate junction temperature value can be calculated by equations (5), (6) and (11) based on lead and case temperatures measured by an infrared camera and thermal resistance values provided in the MOSFET data sheet.

Total power generated inside the silicon and switching losses can be determined by equations (13)-(15).

Literature

[1] www.irf.com/technical-info/designtp/dt99-2.pdf

Designing Automotive LCD Panel Backlight Applications

LEDs are increasingly used as backlight for LCD panels in automotive applications. But under power line surges, electronic modules for automotive applications may suffer from an input voltage of 5 to 7 times higher than nominal. The surge voltage is clamped by external devices like TVS, while the clamped voltage is customer dependent. Electronic engineers always aim at designing electronic modules which can work with a wide input voltage range so that one single design can meet different requirements specified by different customers. This article introduces an LED driver consisting of a boost converter and a 2-channel linear current regulator. **LK Wong, TK Man, Texas Instruments, USA**

DC power in vehicles is provided by a power line which connects all electronic modules powered by the line, a battery, and an alternator driven by the engine of the vehicle. For typical 12 V or 24 V systems, a variation of ±30% in the power line voltage is normally seen. Therefore all electronic modules in automotive applications should take care of such input voltage variation. But during power line surges, the power line voltage rises tremendously. The ISO7637-2 defined pulses 2a and 5a and described some causes of surges (see Table 1). Pulse 2a considers a surge due to sudden interruption of currents in an electronic module powered by the line and the inductances of the wiring harness. Pulse 5a considers a surge due to a load dump transient occurring in the event of a discharged battery being disconnected while the alternator is generating charging current with other loads remaining on the alternator circuit at this moment.

A typical power line voltage profile describing the above surges is shown in Figure 1. It can be seen that the highest power line voltage can be 5 to 7 times of the nominal voltage. Although the duration of surges is not long, only 0.05 ms for pulse 2a and a few hundred milliseconds for pulse 5a, electronic modules connected directly to the power line may be damaged by such a high surge voltage. A common practice is to add an external component like a transient voltage suppressor (TVS) to clamp the peak power line voltage during power line surges. The value of the clamped voltage is customer dependent. However, designers of electronic modules always aim at application circuits which can work with a wide input voltage range so that one single design can suit for different requirements specified by different customers.

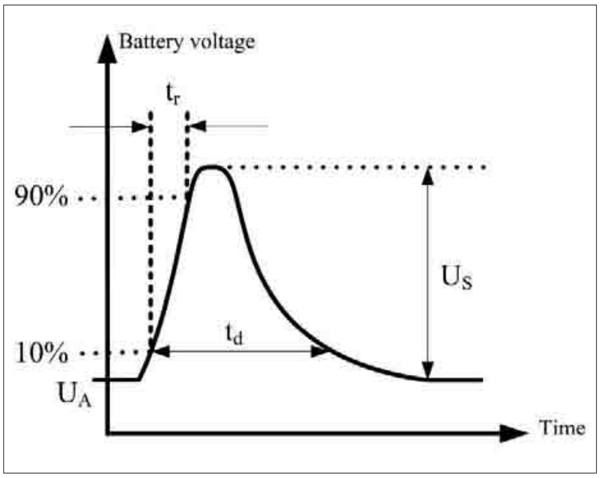

Figure 1: Profile of the power line voltage under surge

LED driver for automotive backlight application

LEDs are increasingly used as backlight for LCD panels in automotive applications because of the fast response time, high contrast ratio, and low power consumption of LEDs. LEDs are in general connecting in series to form a LED string (multiple LED strings can be used for large panels) so that one current regulator can regulate the current of many LEDs. The required driving voltage of a LED string is usually higher than the power line voltage (of 12 V or 24 V systems). In order to step up the power line voltage to drive the LED strings, a boost converter is normally used. A popular architecture of such step-up type LED driver consists of a boost converter and a multi-channel linear current regulator which drives multiple LED strings (as shown in Figure 2). The boost converter consists of an inductor L_1, a switch Q_1, a boost diode D_1 and an output capacitor C_{OUT}.

The input and output voltages are v_{IN} and v_{OUT} respectively. The LED strings 1 to n connects from v_{OUT} to the multi-channel linear current regulator and their forward voltage are represented by V_{LED1} to V_{LEDn}. The current of each LED string is regulated by linear current regulators 1 to n

Pulse	2a		5a
	12V system	24V system	12V system
U_A	13.5V	27V	13.5V
U_S	37V-50V		65V-87V
t_d	0.05ms		40ms-400ms
t_r	9,5µs – 10µs		5ms-10ms

Table 1: Parameters of ISO7637-2 pulses 2a and 5a

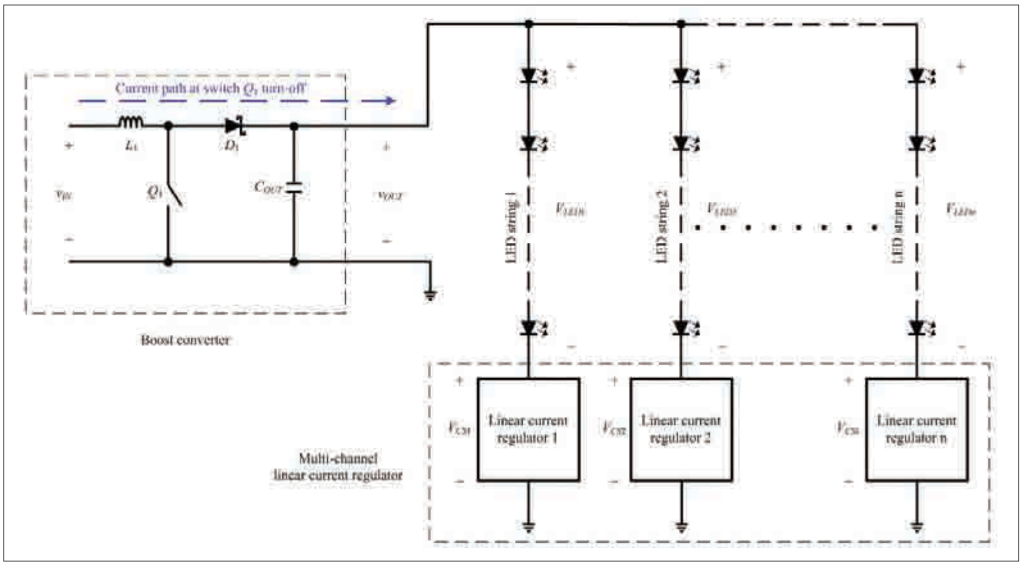

Figure 2: **LED driver with a boost converter and a multi-channel linear current regulator**

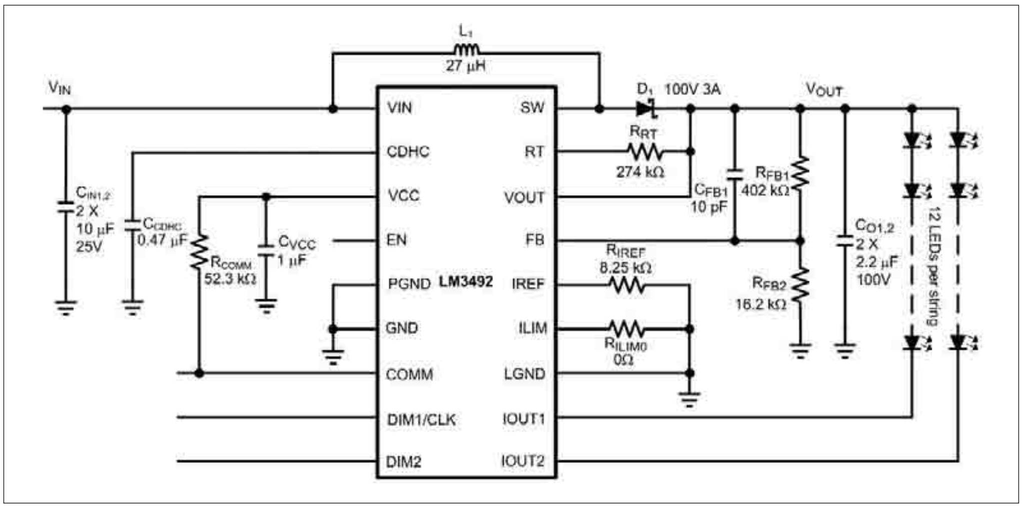

Figure 3: **Schematic of the LM3492 LED driver for automotive LCD panel backlight**

embedded in the multi-channel linear current regulator, and V_{CS1} to V_{CSn} represent the voltage drop on each linear current regulator.

Boost converter under power line surges

Under normal operation, v_{OUT} is regulated to a value which can fully turn on the LED strings and at the same time keep V_{CS1} to V_{CSn} to the minimum. For example, the forward voltage of an LED string (V_{LED1} to V_{LEDn}) with 12 LEDs in series is 38 V, and v_{OUT} can be 39 V if the typical voltage of V_{CS1} to V_{CSn} is 1 V. For 12 V or 24 V systems, v_{OUT} is therefore higher than v_{IN}. But under power line surge, when v_{IN} rise significantly, an abnormal condition that v_{IN} higher than v_{OUT} occurs. A direct response of the boost converter is to stop operation, i.e. to stop the switching of Q_1, and Q_1 stays turned-off. However, the boost diode D_1 is forward biased in this case, the inductor L_1 acts as a short circuit, and consequently a current path still exists (as shown in Figure 2). Hence, v_{OUT} approximately equals $v_{IN,PEAK}$, where $v_{IN,PEAK}$ is the clamped peak power line voltage under surges (depends on the external TVS). It is required that the maximum voltage of the boost controller IC and the drain voltage of the switch Q_1 (either external switch or switch integrated in the IC) should be higher than $v_{IN,PEAK}$. Otherwise, components may be damaged under surges.

An alternative approach to protect the boost converter is to insert a switch between the power line and the boost converter such that the switch turns off if surges detected. The major drawback of this approach is that the LEDs powered by the boost converter must turn off under surges. Therefore this alternative approach is not suitable for a design which is required to meet class A or B of the ISO Failure Mode Severity Classification (all functions of an electronic module perform as designed during and after exposure to interference for class A, and may go beyond the specified tolerance for class B).

Linear current regulator under power line surges

Under power line surges, v_{OUT} can rise to $v_{IN,PEAK}$. But the forward voltage of each LED string (V_{LED1} to V_{LEDn}) remains the same because the LED current, which is still regulated by the linear current regulator, is not affected. As a result, V_{CS1} to V_{CSn} increase significantly. For example, let V_{LED1} and V_{CS1} be 38 V and 1 V respectively under normal operation. If $v_{IN,PEAK}$ is 48 V under surges, V_{CS1} can be 10 V, which is 10 times more than normal. Since the current passing through the linear current regulators remains the same, a sudden increase of V_{CS1} to V_{CSn} drastically increases the power loss; If $v_{IN,PEAK}$ is larger, or V_{LED1} to V_{LEDn} is smaller, V_{CS1} to V_{CSn} is even larger. This increases the power loss of the linear current regulators and damaging may occur. A good design of the linear current regulator should be capable of reducing the regulated current in order to limit the power loss under surges.

Proposed circuit and measured results

A LED driver employing a boost converter and a 2-channel linear current regulator using the LM3492 from Texas Instruments is introduced in Figure 3. The circuit drives two LED strings, each of which consists of

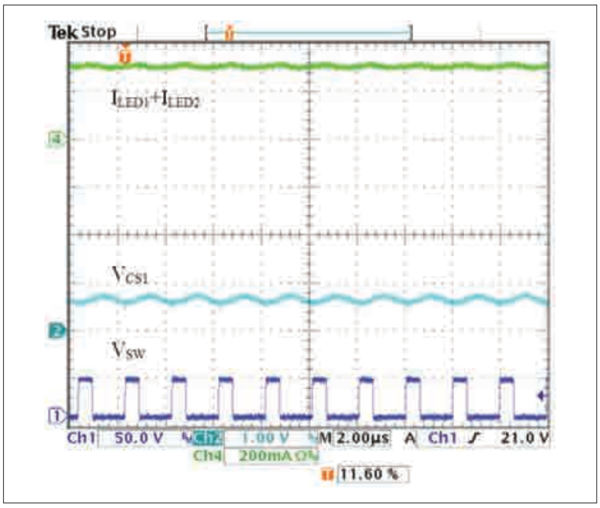

Figure 4: **Waveforms of the LM3492 under a nominal input voltage of 12 V**

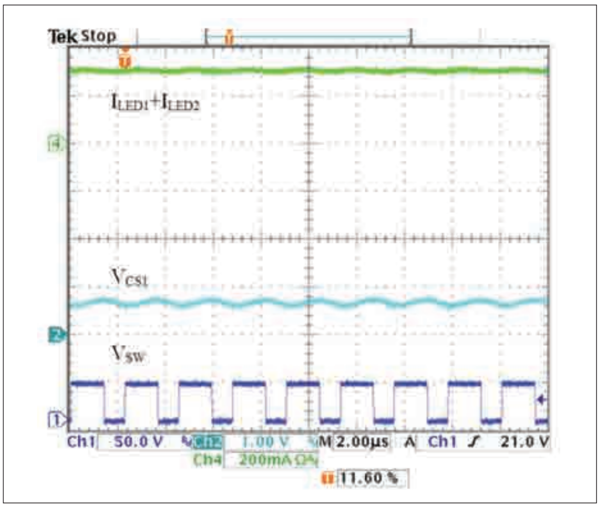

Figure 5: **Waveforms of the LM3492 under a nominal input voltage of 24 V**

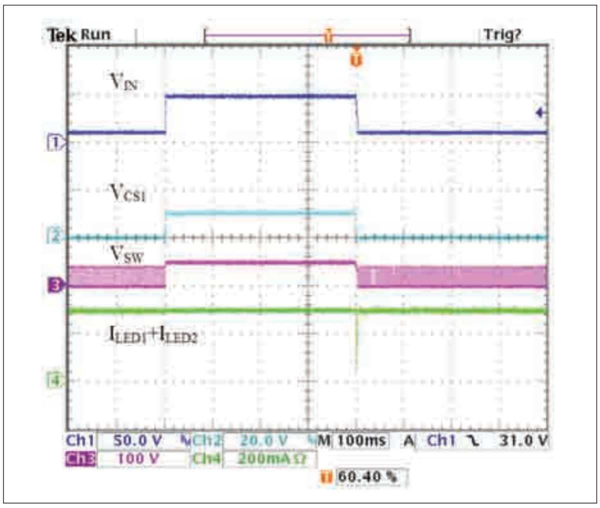

Figure 6: **Waveforms of the LM3492 under a 50 V surge at a nominal input voltage of 12 V**

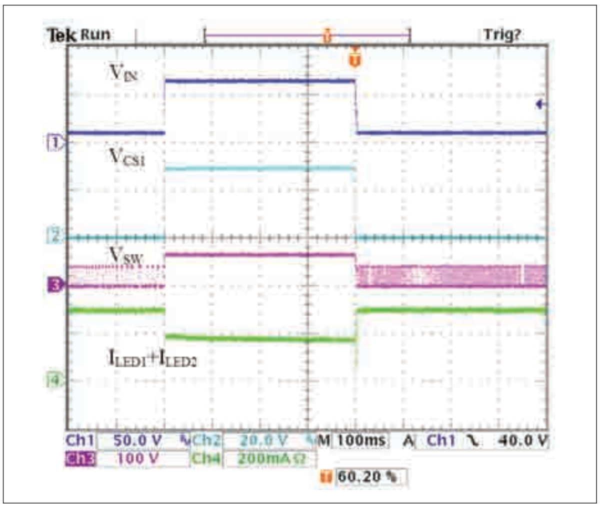

Figure 7: **Waveforms of the LM3492 under a 65 V surge at a nominal input voltage of 12 V**

12 LEDs running at 150 mA, with a nominal LED string forward voltage of 38 V. Figures 4 and 5 show the steady state waveforms of the voltages of the SW, IOUT1 (i.e. V_{CS1}, the voltage drop of the linear current regulator 1) pins of the LM3492 and the total LED current $I_{LED1}+I_{LED2}$ under normal input voltages of 12 V and 24 V respectively. It can be seen that V_{CS1} is below 1 V. Under surges with $V_{IN,PEAK}$ of 50 V (Figure 6), the boost converter stops operation (no switching is seen in the V_{SW} waveform). The total LED current remains unchanged, but V_{CS1} rises to about 9 V, meaning that the power loss is 9 times larger. When V_{IN} drops from the peak to the nominal, the boost converter is usually not turned on fast enough so that a small dip in the LED current is seen. If $V_{IN,PEAK}$ is increased to 65 V (Figure 7), V_{CS1} further rises to 27 V, but the total LED current is reduced to around 200 mA (i.e. 100 mA for each channel instead of 150 mA) by the internal over-power protection circuit in order to protect the linear current regulator.

Conclusion

LEDs are increasingly used as backlight for LCD panels in automotive applications. But under power line surges, electronic modules for automotive applications may suffer from an input voltage of 5 to 7 times higher than nominal. By applying a LED driver consisting of a boost converter and a 2-channel linear current regulator using the LM3492, the LED strings can still operate under surges, showing that the design can meet class A and B of the ISO Failure Mode Severity Classification. Waveforms of the introduced circuit u nder normal operation and surges are shown.

AC/DC Connverters

www.irf.com
International Rectifier Co. (GB) Ltd
Tel: +44 (0)1737 227200

Busbars

www.auxel.com
Auxel FTG
Tel: +44 (0)7714 699967

Capacitors

www.powersemiconductors.co.uk
Power Semiconductors Ltd
Tel: +44 (0)1727 811110

Certification

www.productapprovals.co.uk
Product Approvals Ltd
Tel: +44 (0)1588 620192

Connectors & Terminal Blocks

www.auxel.com
Auxel FTG
Tel: +44 (0)7714 699967

DC/DC Converters

www.irf.com
International Rectifier Co. (GB) Ltd
Tel: +44 (0)1737 227200

DC/DC Connverters

www.power.ti.com
Texas Instruments
Tel: +44 (0)1604 663399

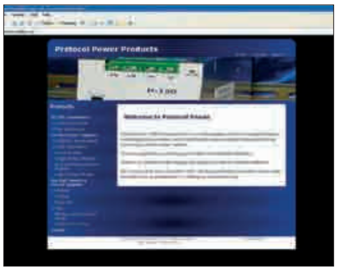

www.protocol-power.com
Protocol Power Products
Tel: +44 (0)1582 477737

Diodes

www.irf.com
International Rectifier Co. (GB) Ltd
Tel: +44 (0)1737 227200

www.mark5.com
Mark 5 Ltd
Tel: +44 (0)2392 618616

www.microsemi.com
Microsemi
Tel: 001 541 382 8028

www.neutronltd.co.uk
Neutron Ltd
Tel: +44 (0)1460 242200

www.voltagemultipliers.com
Voltage Multipliers, Inc.
Tel: 001 559 651 1402

www.proton-electrotex.com/
Proton-Electrotex JSC/
Tel: +7 4862 440642;

Direct Bonded Copper (DPC Substrates)

www.curamik.co.uk
curamik® electronics GmbH
Tel: +49 9645 9222 0

Discrete Semiconductors

www.digikey.com/europe
Digi-Key
Tel: +31 (0)53 484 9584

www.irf.com
International Rectifier Co. (GB) Ltd
Tel: +44 (0)1737 227200

www.mark5.com
Mark 5 Ltd
Tel: +44 (0)2392 618616

www.microsemi.com
Microsemi
Tel: 001 541 382 8028

Drivers ICS

www.irf.com
International Rectifier Co. (GB) Ltd
Tel: +44 (0)1737 227200

www.power.ti.com
Texas Instruments
Tel: +44 (0)1604 663399

Fuses

www.powersemiconductors.co.uk
Power Semiconductors Ltd
Tel: +44 (0)1727 811110

GTO/Triacs

www.mark5.com
Mark 5 Ltd
Tel: +44 (0)2392 618616

Hall Current Sensors

www.dgseals.com
dgseals.com
Tel: 001 972 931 8463

Harmonic Filters

www.murata-europe.com
Murata Electronics (UK) Ltd
Tel: +44 (0)1252 811666

IGBTs

www.irf.com
International Rectifier Co. (GB) Ltd
Tel: +44 (0)1737 227200

www.mark5.com
Mark 5 Ltd
Tel: +44 (0)2392 618616

www.microsemi.com
Microsemi
Tel: 001 541 382 8028

www.neutronltd.co.uk
Neutron Ltd
Tel: +44 (0)1460 242200

www.irf.com
International Rectifier Co. (GB) Ltd
Tel: +44 (0)1737 227200

www.power.ti.com
Texas Instruments
Tel: +44 (0)1604 663399

Magnetic Materials/Products

www.rubadue.com
Rubadue Wire Co., Inc.
Tel. 001 970-351-6100

Mosfets

www.irf.com
International Rectifier Co. (GB) Ltd
Tel: +44 (0)1737 227200

www.mark5.com
Mark 5 Ltd
Tel: +44 (0)2392 618616

www.microsemi.com
Microsemi
Tel: 001 541 382 8028

www.neutronltd.co.uk
Neutron Ltd
Tel: +44 (0)1460 242200

Optoelectronic Devices

www.digikey.com/europe
Digi-Key Tel: +31 (0)53 484 9584

www.power.ti.com
Texas Instruments
Tel: +44 (0)1604 663399

Packaging & Packaging Materials

www.curamik.co.uk
curamik® electronics GmbH
Tel: +49 9645 9222 0

Power ICs

www.digikey.com/europe
Digi-Key Tel: +31 (0)53 484 9584

www.irf.com
International Rectifier Co. (GB) Ltd
Tel: +44 (0)1737 227200

www.power.ti.com
Texas Instruments
Tel: +44 (0)1604 663399

Power Modules

www.auxel.com
Auxel FTG
Tel: +44 (0)7714 699967

www.irf.com
International Rectifier Co. (GB) Ltd
Tel: +44 (0)1737 227200

www.mark5.com
Mark 5 Ltd
Tel: +44 (0)2392 618616

www.microsemi.com
Microsemi
Tel: 001 541 382 8028

www.power.ti.com
Texas Instruments
Tel: +44 (0)1604 663399

www.proton-electrotex.com/
Proton-Electrotex JSC/
Tel: +7 4862 440642;

Power Protection Products

www.power.ti.com
Texas Instruments
Tel: +44 (0)1604 663399

Power Semiconductors

www.proton-electrotex.com/
Proton-Electrotex JSC/
Tel: +7 4862 440642;

Power Substrates

www.universal-science.com
Universal Science Ltd
Tel: +44 (0)1908 222211

Resistors & Potentiometers

www.isabellenhuette.de
Isabellenhütte Heusler GmbH KG
Tel: +49/(27 71) 9 34 2 82

RF & Microwave Test Equipment.

www.ar-europe.ie
AR Europe
Tel: 353-61-504300

Simulation Software

www.power.ti.com
Texas Instruments
Tel: +44 (0)1604 663399

www.universal-science.com
Universal Science Ltd
Tel: +44 (0)1908 222211

Smartpower Devices

www.irf.com
International Rectifier Co. (GB) Ltd
Tel: +44 (0)1737 227200

Switches & Relays

www.irf.com
International Rectifier Co. (GB) Ltd
Tel: +44 (0)1737 227200

Switched Mode Power Supplies

www.biaspower.com
Bias Power, LLC
Tel: 001 847 215 2427

Switched Mode Power Supplies

www.power.ti.com
Texas Instrumments
Tel: +44 (0)1604 663399

Thermal Management & Heatsinks

www.abl-heatsinks.co.uk
ABL Components Ltd
Tel: +44 (0) 121 789 8686

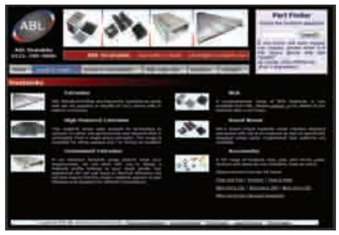

www.curamik.co.uk
curamik® electronics GmbH
Tel: +49 9645 9222 0

www.dau-at.com
Dau GmbH & Co KG
Tel: +43 3143 23510

www.lairdtech.com
Laird Technologies Ltd
Tel: 00 44 1342 315044

www.power.ti.com
Texas Instrumments
Tel: +44 (0)1604 663399

www.universal-science.com
Universal Science Ltd
Tel: +44 (0)1908 222211

Thyristors

www.irf.com
International Rectifier Co. (GB) Ltd
Tel: +44 (0)1737 227200

www.mark5.com
Mark 5 Ltd
Tel: +44 (0)2392 618616
www.proton-electrotex.com/
Proton-Electrotex JSC/
Tel: +7 4862 440642;

Voltage References

www.irf.com
International Rectifier Co.
(GB) Ltd
Tel: +44 (0)1737 227200

ADVERTISERS INDEX

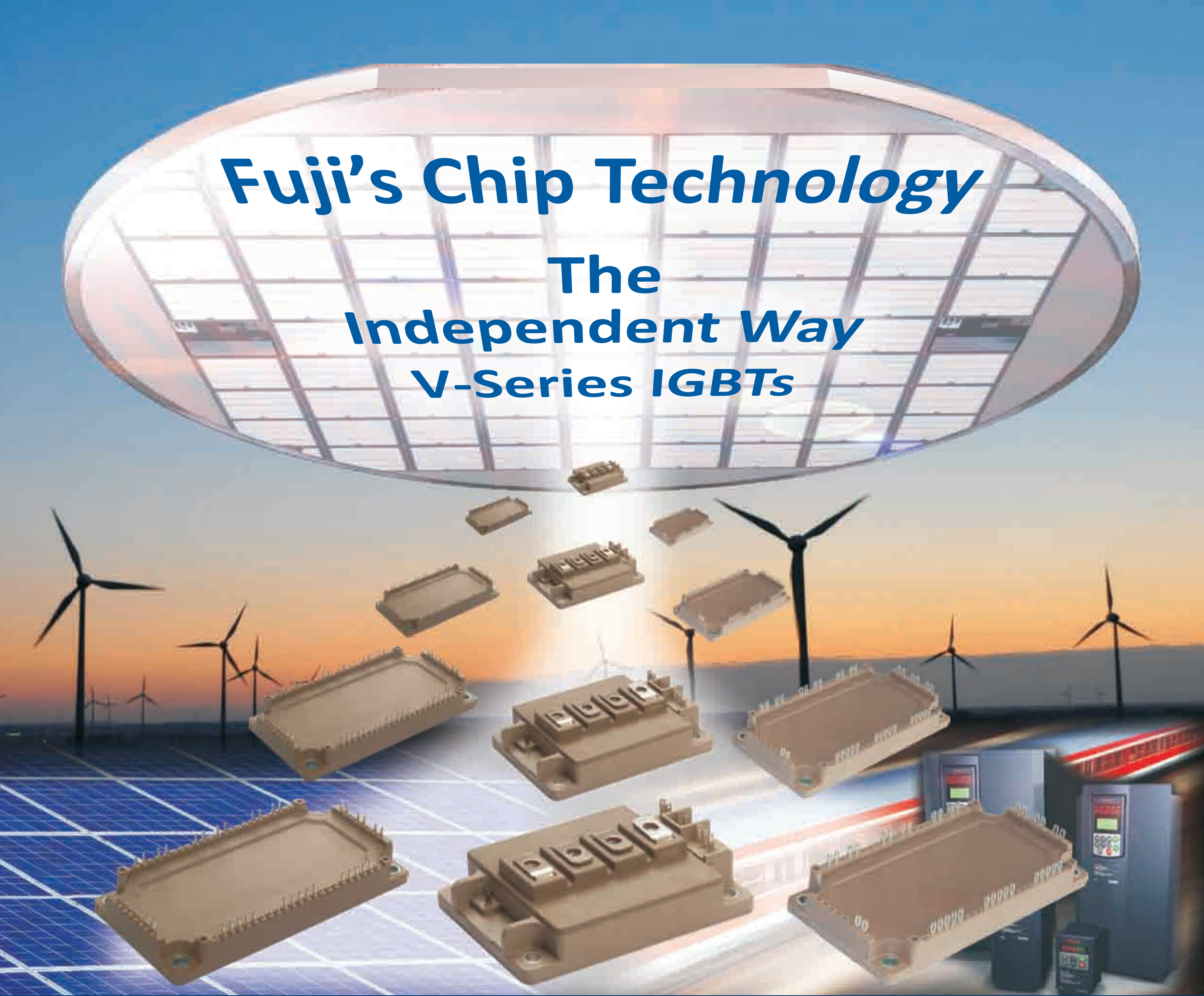

• Trench-FS IGBT • High thermal cycling capability • Low spike voltage & oscillation free • Excellent turn-on dI_C/dt control by R_G

Innovative Reverse-Blocking IGBT for 3-Level inverters with T-configuration

1 phase IGBT modules

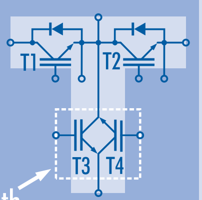

Advanced solution with Reverse-Blocking-IGBT

	T1 & T2	T3 & T4
200A*)	1700V	1200V
300A	1200V	600V
400A	600V	600V

*) Under development

3 phase IGBT modules

With solder pins

With PressFit contacts

Advanced solution with Reverse-Blocking-IGBT

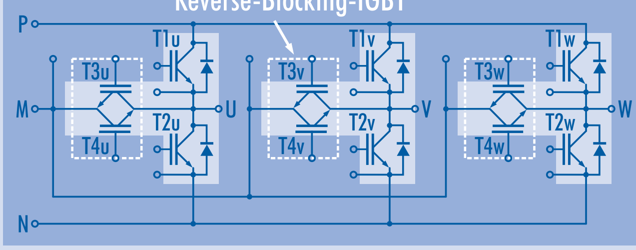

	T1 & T2	T3 & T4
50A	1200V	600V
75A	1200V	600V
100A	1200V	600V

Fuji Electric
Innovating Energy Technology

Fuji Electric Europe GmbH
Goethering 58 · 63067 Offenbach am Main · Germany
Fon +49(0)69-66 90 29 0 ▸semi-info@fujielectric.de
Fax +49(0)69-66 90 29 56 ▸www.fujielectric.de
Products Overview ▸ www.fujielectric-europe.de/info/overview.pdf

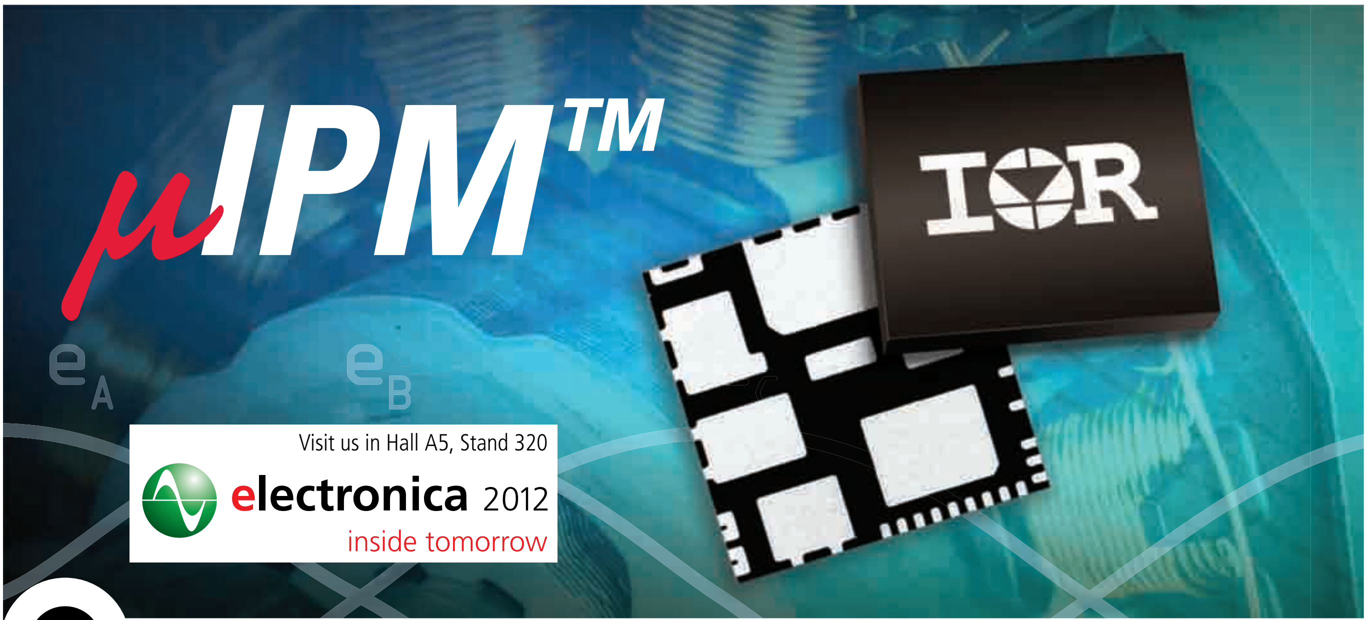

Innovative Power Module Reduces System Size

μIPM™ Power Modules Deliver up to 60% Smaller Footprint

Specifications:

Part Number	Size (mm)	Voltage	IO (DC@ 25°C)	Motor Current**		Motor Power VO=150/75VRMS	Topology
				w/o HS	w/HS		
IRSM836-024MA	12x12	250V	2A	470mA	550mA	60W/72W	3P Open Source
IRSM836-044MA	12x12	250V	4A	750mA	850mA	95W/110W	3P Open Source
IRSM836-025MA	12x12	500V	2A	360mA	440mA	93W/114W	3P Open Source
IRSM836-035MB	12x12	500V	3A	420mA	510mA	108W/135W	3P Common Source
IRSM836-035MA	12x12	500V	3A	420mA	510mA	100W/130W	3P Open Source
IRSM836-045MA	12x12	500V	4A	550mA	750mA	145W/195W	3P Open Source

Features:

- 3-phase motor control IC
- 12x12x0.9mm PQFN package offers up to 60% smaller footprint
- Eliminates the need for heat sink
- DC current ratings from 2A to 4A
- Voltage range of 250V – 500V

μIPM™ Advantages:

- Shortens design time
- Shrinks board space requirements
- Simplicity - Eliminates Heat Sink
- Replaces more than 20 discrete parts to deliver a complete motor drive stage
- Slashes assembly time and cost
- Simplifies procurement and inventory management
- Reference design kits available for quick evaluation on any 3-phase motor

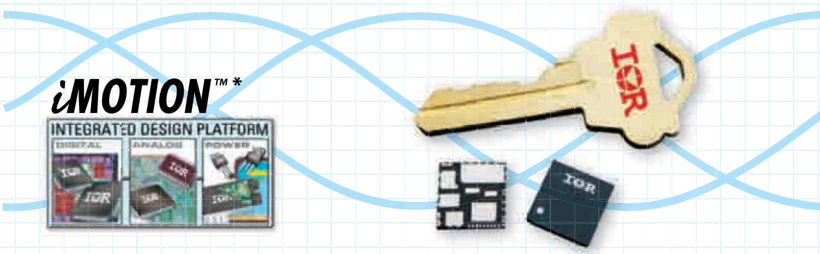

For more information call +49 (0) 6102 884 311
or visit us at www.irf.com

International Rectifier
THE POWER MANAGEMENT LEADER

* IR's iMOTION™ (ai mo shan), representing the intelligent motion control, is a trademark of International Rectifier
** RMS, Fc=16kHz, 2-phase PWM, TCA=70°C, TA 25°C